学 位 論 文

Magma genesis of continental flood basalts: A case study of Deccan Trap basalts, India

洪水玄武岩のマグマ成因論：インド・デカントラップを例とした研究

平成8年12月博士（理学）申請

東京大学大学院理学系研究科地質学専攻

佐 野 貴 司

Magma genesis of continental flood basalts: A case study of Deccan Trap basalts, India

Takashi Sano

University of Tokyo

December, 1996

Abstract

This thesis presents new geological and petrological information for Deccan Trap province, India. Magma genesis of Large Igneous provinces (LIPs) has been discussed based on the geological and petrological information.

Based on the geological and geochemical study of basalt flows exposed in several sections located in the Western Ghats area, eleven formations were recognized among twelve formations which were previously established. In central and eastern Deccan, an attempt has been made to divide the lava piles into different stratigraphic group. Further, it has also been attempted to compare these groups with the formations of the western Deccan. Chemical analogous of the Poladpur, Ambenali and Mahabaleshwar Formations of the Western Ghats have been recognized in the central and eastern Deccan. For the purpose of establishing the chemical stratigraphy, two distinctive chemical groups have been identified in the central and eastern Deccan. These two key groups have a large regional extent in the central and eastern areas, and are named as Eastern Ambenali Formation and Eastern Low-Ti Formation. Eastern Low-Ti Formation overlies Eastern Ambenali Formation. The chemical signature and stratigraphic relations favor the fact that Eastern Ambenali Formation corresponds to Ambenali Formation in the Western Ghats area. Moreover, Eastern Low-Ti Formation may correspond to Panhala or Desur Formation in the Western Ghats area.

Some of Deccan Traps magmas probably suffered significant amount of contamination by lithosphere en route to the surface, because they erupted through thick continental lithosphere. In order to avoid this effect for discussing the magma genesis of Deccan Trap basalts, uncontaminated basalts were selected. The uncontaminated basalts in whole Deccan Traps could be discriminated based on the Ba/Nb ratio and TiO_2 composition. The uncontaminated basalts form thick lava pile (> 500 m) which is defined as Ambenali Formation in the Western Ghats area. Total volume of the uncontaminated basalts is estimated at 51 % in whole Deccan Traps.

The uncontaminated basalts form a distinct chemical trend. This chemical trend was evaluated with the aid of the one atmosphere melting experiments at controlled oxygen fugacity conditions on QFM and NNO buffers, such that the fractional crystallization at low pressure and at relatively reducing condition (QFM buffer) explains well the chemical trend of the uncontaminated basalts. Temperature interval of crystallization was estimated to be 1155-1130 °C. One of the most evolved uncontaminated basalts can be generated by removal of phenocrystic phases (olivine = 4 wt.%, plagioclase = 16 wt.%, augite = 15 wt.%) from the most primitive basalt. The most primitive aphyric basalt in the uncontaminated basalts is related to the pristine magma of Deccan Traps.

The pristine magma of Deccan Traps is tholeiite and primitive mantle normalized La/Lu ratio, $(La/Lu)_N$, of more than 2.2. Based on the review of the previous melting experiments, numerical simulations of partial melting of mantle lherzolite and subsequent fractional crystallization have been conducted to evaluate whether or not the pristine magma can be derived from typical mantle lherzolite (primitive and MORB-source mantle). In order to generate tholeiitic magma, the degree of partial melting must be high enough. On the other hand, the degree of partial melting must be low so as to generate magma which has high $(La/Lu)_N$ such as 2.2. This quantitative examinations implies that any tholeiitic magma with $(La/Lu)_N$ more than 2.2 can not be derived from mantle lherzolite.

As it was shown that mantle lherzolite is not appropriate for the source of the Deccan pristine magma, a composite plume which is composed of subducted oceanic crust and mantle lherzolite has been examined as a probable source material. For the purpose, melting experiments have been conducted on an abyssal tholeiite from the Mid-Atlantic Ridge at pressures between 3 and 5.5 GPa using diamond aggregate method, because experimental studies on the composition of partial melt of basalts at high pressure were quite scarce. The experimental results showed that the liquidus phase is clinopyroxene followed by garnet at the pressure range in this study. Obtained compositions of partial melts coexisting with these residual phases were used to apply the composite plume model to the genesis of Deccan magma.

In the application of the composite plume model, the alkalic picrite from Kathiawar area in Deccan Traps is considered to be a representative of partial melt of the host lherzolite. That picrite erupted simultaneously with the Deccan Trap tholeiite, and its composition suggests it can be equilibrated with mantle lherzolite. It was also assumed that segregation of the magma from basaltic blocks within the composite plume to mix with the partial melt of the ambient lherzolite and to form hybrid magma occurred at the same pressure where the picrite magma segregated from the ambient lherzolite of the composite plume. The pressure and temperature conditions for melt segregation to satisfy the rare earth element compositions of the alkalic picrites is estimated through inversion calculations using elemental partitioning data. Thus obtained condition is 2.8 GPa and 1410 °C .

Next, assuming that the hybrid magma correspond to the pristine magma of Deccan Traps, weight fraction of basaltic blocks or layers in the composite plume was estimated based on batch melting model using rare earth element compositions. The mixing ratio, M_B/M_P, of basaltic blocks or layers and the ambient lherzolite part in the composite plume was calculated to be 0.05-0.09. The major and trace element composition of the hybrid magma calculated using the above estimated pressure, temperature and mixing ratio (M_B/M_P) in the composite plume is akin to that of the pristine magma. Therefore, it can be concluded that the pristine magma of Deccan Traps can be explained by the composite plume model.

Contents

Illustrations

List of figures

List of tables

I. Introduction

Large igneous provinces (LIPs) are continua of voluminous mafic rock emplacements which originate via processes other than normal sea-floor spreading (Coffin and Eldholm, 1994). Coffin and Eldholm (1994) examined previous studies and suggested that after basalt and associated intrusive rock emplaced at spreading centers, LIPs are the most significant accumulations of mafic materiel on the Earth's surface. LIPs, therefore, provide windows into those regions of the mantle. LIPs are characterized by their large volume and high eruption rates (*e.g.*, Kent *et. al.*, 1992). From this point of view, it has been suggested that LIPs are commonly attributed to mantle plumes or hot spot. Some different physical models have been proposed to explain the genesis of all LIPs or individual LIP (*e.g.*, Griffiths and Campbell, 1991; White and McKenzie, 1989). However, these models were not exactly evaluated by petrological studies, because only a few geological and geochemical data were reported for LIPs. LIPs are so large that it is difficult to collect representative geological and geochemical data. Moreover, because of their old ages (pre-Quaternary), the serious effects of erosion and alteration also make hard to collect the geological data.

Deccan Traps province of India represents one of the largest LIPs and has attracted attention of the geoscientists from world over. Many scientists have investigated the Deccan Traps province and many geological and geochemical data have been accumulated. This is one of the most appropriate provinces to investigate the magma genesis of LIPs from petrological aspect.

Most of geological investigations were confined to the better exposed parts of the Deccan in the West, which offer thick sections of lava pile for examination. Stratigraphy of the Western Ghats area has been established by previous workers (Beane *et al.*, 1986; Bodas *et al.*, 1988; Cox and Hawkesworth, 1984, 1985; Devey and Lightfoot, 1986; Khadri *et al.*, 1988; Mitchell and Cox, 1988; Lightfoot *et al.*, 1990). Geological map has been also published in the Western Ghats area (*e.g.*, Subbarao and Hooper, 1988). On the contrary, geological studies of central and eastern areas have not been examined in

such great details. Subbarao *et al.* (1994) has recently published the possible stratigraphy in these areas, however, their works have restricted only the central area. Other investigations of these areas are also essentially restricted to few and far apart area (Allmukhamedov and Zolotukhin, 1988; De, 1994; Nair and Roi, 1994; Sen and Cohen, 1994; Srivastava *et al.*, 1988). Stratigraphic framework for the central and eastern parts is yet to be firmly established. Hence, continuity of all or some of the formations from west into central and eastern parts is not known with certainty. Therefore, I propose the possible stratigraphy of lava pile in the whole Deccan Traps province including central and eastern area.

Many petrological studies have been reported about the Deccan basalts in Western Ghats area. Previous workers investigated the process to explain the chemical variations of whole rock and mineral compositions of basalts in Western Ghats area. They concluded that chemical variations of the least contaminated magma, Ambenali magma, could be explained by low pressure fractional crystallization process. However, it is not clear if the similar arguments are applicable to the basalt piles in the central and eastern parts of Deccan. Moreover, there is no petrological study to evaluate the physical model to explain magma genesis of Deccan Traps.

In this thesis, therefore, following discussions are presented. (1) The possible stratigraphy of whole Deccan Traps province is proposed based on morphological, petrographical and geochemical characteristics of lava flows. (2) The uncontaminated basalts are distinguished among the basalts in whole Deccan Traps and compositional variation within the uncontaminated basalts is discussed based on the one atmosphere melting experiments. (3) In order to evaluate the physical models to explain magma genesis of LIPs, petrological investigations are done based on the high pressure melting experiments.

II. Geological Setting

1. Distribution of the Deccan Traps

The Deccan Traps of Peninsular India form one of the most extensive continental tholeiitic flood basalt province of the world, covering more than 500,000 km^2 (Fig. 2.1). It has been suggested that a large volume of the Deccan Trap lava flows have been encountered in offshore under Arabian sea. The basalts were erupted through dominantly Precambrian continental crust, much of it Archean onto the Indian continent.

The basalt flows, in general, are thick, tabular in form and broadly horizontal in disposition. They exhibit gentle gradients of less than 1° in different directions. Steeper dips exceeding 5° are noted in structurally disturbed areas (Raja Rao *et al.*, 1978). The lava sequence is thinnest in the east, such as 10 m at Nagpur and thickens westward to more than 2000 m in the Western Ghats (Deshmukh *et al.*, 1977). The maximum exposed thickness is > 1.7 km in the Igatpuri-Kalsubai area in the Western Ghats near Bombay and Nasik. Some lava flows are traceable over distance well in excess of 100 km with no signs of dying out (Beane *et al.*, 1986).

The total volume of effused lava estimated exceeds 1×10^6 km^3 (Deshmukh, 1982). The original volume, prior to erosion and including their continuation beneath the Arabian sea was estimated upward to 1.5×10^6 km^3 (Mahoney, 1988).

2. Age constrains

Prior to 1980, all radiometric dating determinations for Deccan Trap basalts were carried out by K-Ar method (*e.g.*, Kaneoka and Haramura, 1972). However, due to inherent limitations of K-Ar method it is not possible to precisely determine the ages due to argon loss resulting on account of alteration. The technique of ^{40}Ar- ^{39}Ar plateau age is the more efficient to determine the effect of excess argon or argon loss. Therefore, exact

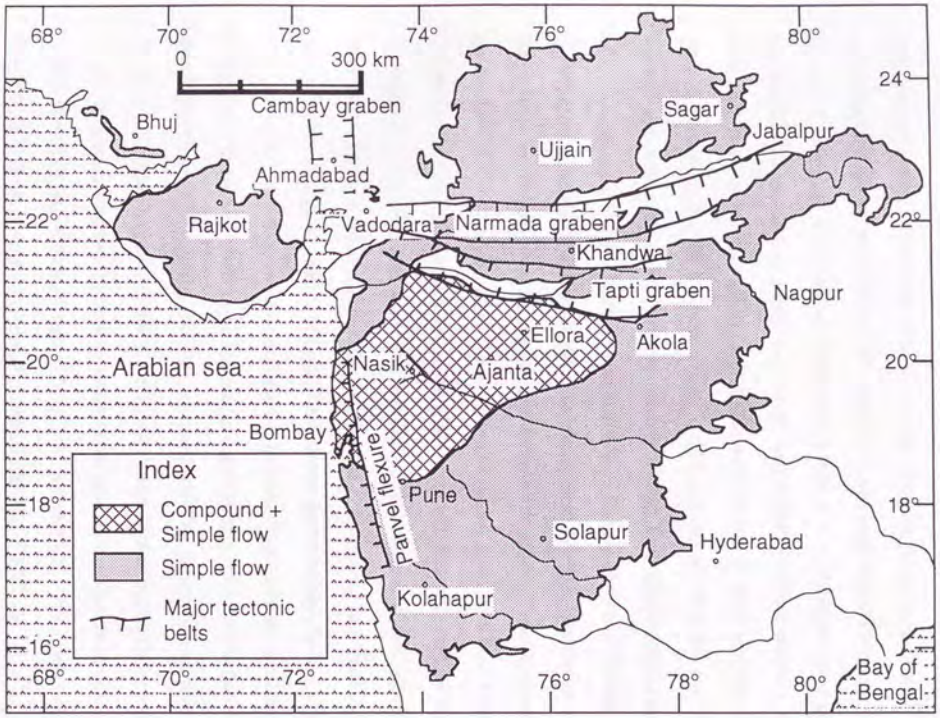

Fig. 2.1 Geological map of Deccan Traps and location of the main tectonic belts (after Bhattacharji *et al.*, 1994; Deshmukh, 1988).

age determinations were carried out after 1980 (Baksi, 1994; Courtillot *et al.*, 1988; Duncan and Pyle, 1988; Kaneoka, 1980; Vandamme *et al.*, 1991; Venkatesan *et al.*, 1993) using ^{40}Ar-^{39}Ar technique.

Venkatesan *et al.* (1993) reported ^{40}Ar-^{39}Ar plateau ages of basalt samples representing over 2.5 km thick lava pile in the Western Ghats area (Fig. 2.1). They suggested that bulk of the basalts of Western Ghats area were erupted between 67 and 62 Ma, and that overall duration may have been at least 3 m.y.. However, they concluded that the lower 2 km thick reversely magnetized lava sequence erupted within 1 m.y. close to 67 Ma. Vandamme *et al.* (1991) reported that the spread of more reliable ^{40}Ar-^{39}Ar ages is between 68 and 63 Ma with a peak at 65.5 ± 2.5 Ma and that this age consistent with the age of the Cretaceous-Tertiary boundary (KTB). They also suggested that almost of all the igneous activity occurred in less than 1 m.y.. Baksi (1994) and Duncan and Pyle (1988) came to similar conclusion, that most basalts from Western Ghats were erupted in less than 1 m.y. For the areas away from the Western Ghats area, Courtillot *et al.* (1988) reported ^{40}Ar-^{39}Ar plateau ages of five samples which were collected from widely separated regions in the Deccan Traps. They also concluded that the bulk of the Deccan eruptions occurred in a short time (less than 1 m.y.). Iwata (*pers. comm.*) considers that effusion of the main volume of Deccan Trap basalts is restricted to a period of < 2 m.y., as constrained by a large number of ^{40}Ar-^{39}Ar plateau ages of basaltic lava samples.

The short period of volcanic activity for Deccan Trap could be confirmed by the geological information, such as the absence of intertrappean thick sedimentary layers in many thick sections and the lack of erosional profiles which developed between successive eruption (*e.g.*, Deshmukh, 1977). The intertrappean beds which mostly occur in the peripheral regions of Deccan outcrop are mainly composed of ashes or lake sediments which are both characterized by of high sedimentation rate, and consequently, they were deposited during short period of time (Mahoney, 1988).

Paleontological data and magnetostratigraphic observations (*e.g.*, Courtillot *et al.*, 1986) on the Deccan Trap basalts have been reviewed by Vandamme *et al.* (1991). They concluded that these results are consistent with the radiometric ages as follows;

combination of stratigraphic mapping with the magnetic measurements suggested that almost all volcanism took place within reversed chron 29 R, which includes the KTB, paleontological data on intertrappean and intertrappean sediments constrained Deccan age between about 67 and 60.5 Ma.

These age data represent extremely rapid eruption rates such as 1 km^3/yr., when almost total volume (about 10^6 km^3) of Deccan basalt was effused within 1 Ma.

3. Plate tectonic reconstruction

Plate tectonic reconstruction indicates that the Indian continent migrated northward after its separation from the Madagascar island around 80 Ma (Norton and Sclater, 1979; Scotese *et al.*, 1988) (Fig. 2.2). Subsequently, the northern part of Indian continent collided against the southern Asian continent shortly before the KTB (Klootwijk *et al.*, 1992).

It has been reported that the Deccan Traps were extruded at the same time as the Seychelles bank rifted away from Indian continent, close to the time of the KTB (Norton and Scalar, 1979; Müller *et al,* 1993; Vink *et al.*, 1984). This separation has been interpreted to have been caused due to a ridge jump by the Indian continent during its northward migration as it passed over a plume which is situated beneath the present site of Reunion island located (Morgan, 1981). The trace of the hot spot now believed to be located beneath the Reunion island could be traceable as follows (Fig. 2.3); after the eruption of the Deccan Trap basalts, the Laccadives, Maldives and Chagos Bank were formed as the Indian plate migrated northward with respect to the hot spot which assumed fixed position in the mantle, following this Carlsberg Ridge oceanic spreading centre passed the plume and the plate continued to migrated northward, generating the Mauritius and Réunion (Morgan, 1981; Müller *et al.*, 1993).

Klootwijk *et al.* (1992) proposed that the deformation of the Indian continent along two major fault systems may have occurred when stresses were originated by the contact

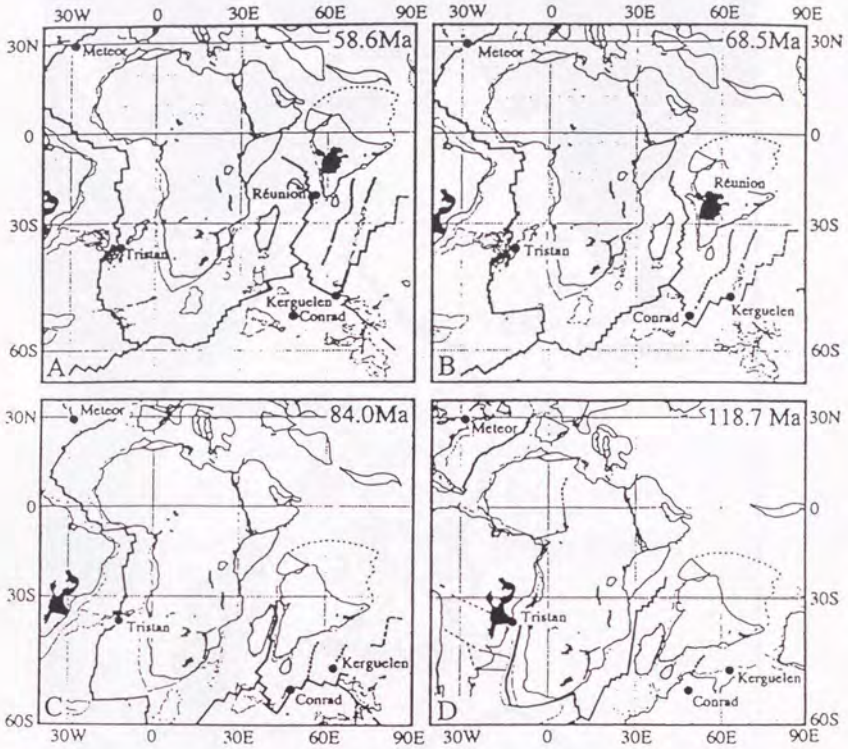

Fig. 2.2 Reconstruction of plates relative to major Atlantic and Indian ocean hot spots from Müller *et al.* (1993). Solid circles are present locations of hot spots. Black areas are flood basalts. The Deccan Traps were erupted through the Indian continent after separating from the Madagascar island.

Fig. 2.3 Present geography of the west Indian Ocean showing the volcanic trace of the Reunion hotspot as it migrated southwestward away from its initial position under the Indian continent, after Müller *et al.* (1993). Open circle with number indicates radiometric ages (Ma) compiled by Müller *et al.* (1993).

of the two continents (Asia and India). These two fault systems are the Panvel flexure along the west coast of Peninsula India and Tapti and Narmada grabens (Fig. 2.1). The magma generated at the mantle may have moved smoothly to the surface along these tectonic generated faults.

The velocity of migration of the Indian plate was estimated to be about 14-20 cm/yr. during most of the period of Deccan Trap eruptions (Kent *et al.*, 1992).

4. Topography, structure and tectonics of Deccan Traps

Maximum thickness of Deccan basalts is exposed in the Western Ghats and Satpura maintains and also in adjoining Tapti and Narmada river regions. Thickness of lava pile is more than 2000 m in the Western Ghats, while it exceeds 1000 m in the Satpura-Tapti and Narmada regions (Deshmukh, 1977). The drainage pattern also indicates that crest of Western Ghats and rift of Tapti and Narmada are the watershed for most of peninsular India (Cox 1989).

The geological and geophysical evidences indicate presence of major tectonic belts along the west coast and along Tapti and Narmada lineament zone. These tectonic belts are characterized by the Panvel flexure and Tapti and Narmada grabens (Kaila, 1988). A large number of dykes occur in swarms both in the Western Ghats and along the west coast and also in Tapti and Narmada rift regions (Deshmukh and Sehgal, 1988). The tectonic belts extend for several hundred kilometers and most of the faults and fractures follow these trends (Kailasam *et al.*, 1977). Tapti and Narmada grabens are characterized by presence of step normal faults. The crustal area along these grabens is faulted and fractured, some of these linearments being deep enough to reach the mantle (Kaila, 1988; Verma and Banerjee, 1992). The two tectonic belts are also the sites of positive gravity anomalies and high thermal gradients (Kailasam *et al.*, 1972; Gupta and Gaur, 1984; Verma and Banerjee, 1992).

Most dikes along the tectonic belts are of mafic hypabyssal type with a minor proportion of them being alkalic, acidic, or ultramafic in composition. Mafic dikes occur in clusters and swarms in the two regions paralleling the N-S trending Western Ghats and E-W trending Narmada and Tapti grabens. In Narmada-Tapti belt more than 80 percent of the dikes are aligned parallel to major E-W tectonic trend, whereas less than 50 percent dikes in the west coast region follow the N-S trend (Deshmukh and Sehgal, 1988). Most dikes are traceable only over short distances (just a few hundred meters), while, some of them are seen to extend to 70 km or more. They very in width from 0.5 to 100 m, however, majority of the dikes ranges in width from 5 to 20 m (Deshmukh and Sehgal, 1988; Godbole and Ray, 1992; Nair and Chatterjee, 1993).

Though dykes occur in profusion, only a few have been considered to be the likely source for extensive lava flows (Mahoney, 1988). Dykes exhibiting characters of eruptive fissure have been reported from some areas (Deshmukh, 1977, 1988). Paucity of feeder dykes has been interpreted by Deshmukh and Sehgal (1988) due to tendency of lava to sink back into the fissure at the end of eruption. The orientation of large probable feeder dikes in the Western Ghats region (especially between Bombay and Nasik area) is essentially random (Beane *et al.*, 1986). Hooper (1990) suggested that this fact implies that the crust was not under extentional strain when the main phase of the Deccan Trap basalts was erupted. He also concluded that lava flows in the Western Ghats region were effused the shield-type volcanic eruption. For the structural study, it has been observed that the lava flows exhibit southerly dips in the Western Ghats region with overstepping by successively younger formations forwards south (Beane *et al.*, 1986; Devey and Lightfoot, 1986). They also concluded that lava flow structure in Western Ghats may have implied a large shield volcano-type eruption with southerly migrating of the focus of the volcanism.

Two types of basaltic flows have been recognized in the Deccan Traps. They are compound flows and simple flows (Beane *et al.*, 1986; Deshmukh, 1977, 1988; Walker, 1972). Walker (1972) suggested that basaltic lavas extruded at high effusion rates form far-reaching flows composed of a single flow unit, whereas those extruded at low

effusion rates produce flows composed of small flow units which pile up close to the vent and produce compound lavas. Deshmukh (1988) showed that compound flows are mainly extensively developed in the Western part of the Deccan Traps and constitute stratigraphically older sequence compare to the simple flows of this region (Fig. 2.1). Ash layers and pyroclastics also exist in the Western Ghats area (Raja Rao *et al.*, 1978). The existence of both compound flows and ash beds indicates relative proximity to sites of eruption and major foci of magmatic eruption might have been in the Western Ghats region (Mahoney, 1988).

For the eruptions of Tapti and Narmada region, deep seated fault and fracture linearments acted as conduits for the ascending magma (Bhattacharji *et al.*, 1994; Deshmukh and Sehgal, 1988). Bhattacharji *et al.* (1994) proposed that majority of the dikes in Tapti and Narmada grabens occupy tension fractures, along which, magma could have moved smoothly to the present level of erosion. They also reported that dikes are similar in chemical, mineralogical composition and in radiometric ages to the associated sequence of basaltic flows. On this basis, they concluded that the dikes along the Tapti and Narmada grabens acted as primary feeders for the main tholeiitic flows. Moreover, Kent *et al.* (1992) suggested that Tapti and Narmada grabens existed before the main eruptive period of Deccan Trap basalts and as such magma could migrate along these fracture of these grabens. They proposed that pre-eruption crustal stressing occurred because of the mantle plume of the source of the Deccan trap basalts incubated at the base of the lithosphere.

III. Chemical stratigraphy

1. Previous works

A. Western Ghats area

The lava pile forming the Deccan basalts group in the Western Ghats between Nasik and southern edge of the Deccan Traps has been divided into twelve stratigraphic formations (Beane *et al.*, 1986; Bodas *et al.*, 1988; Cox and Hawkesworth, 1984, 1985; Devey and Lightfoot, 1986; Khadri *et al.*, 1988; Lightfoot *et al.*, 1990; Mahoney *et al,* 1982 ; Mitchell and Cox, 1988 Mitchell and Widdowson, 1991). They are Jawhar, Igatpuri, Neral, Thakurvadi, Bhimashankar, Khandala, Bushe, Poladpur, Ambenali, Mahabaleshwar, Panhala and Desur from lower to upper, respectively. These formations have been defined based on both field observations and chemical characters such as major and trace element abundance, inter element ratios, ^{87}Sr-^{86}Sr isotope ratios of lava flows. Fig. 3.1 shows the compiled stratigraphic cross-section of the Western Ghats area after Mahoney (1988). In this figure, we can see the oldest formation of the lava pile is exposed in the Igatpuri area, while younger formations are exposed to the south, displaying overstepping arrangement, caused due to southerly dips of the formation boundaries.

The method of allocation of basalts into upper six formations (upper than Bushe formation) is based on the geochemical criteria established by Cox and Hawkesworth (1984, 1985), Devey and Lightfoot (1986), Lightfoot *et al.* (1990). Each formation is separated from the other by a sharp break in chemical compositions. These criteria, together with new definition of this study are summarized in Table 3.1 (mainly compiling Devey and Lightfoot, 1986 and Lightfoot *et al.*, 1990).

Each formation lower than Thakurvadi Formation (lower six formations) is mainly separated from the others by the megascopic and field observations such as the existence of giant plagioclase phenocrysts basalt (GPB) horizon at or near the formation boundary

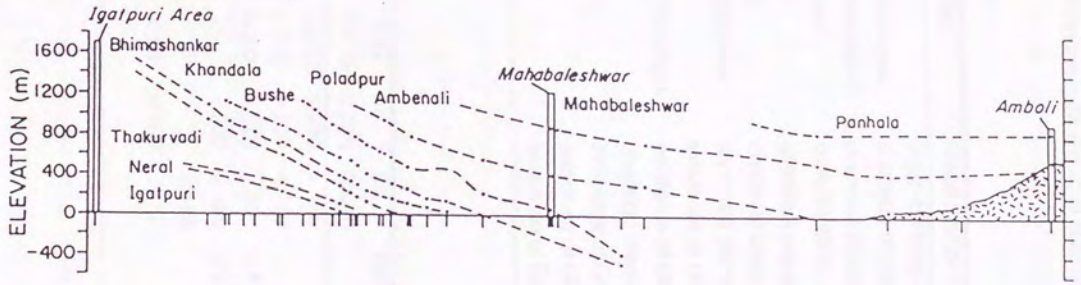

Fig. 3.1 N-S stratigraphic cross-section of the Western Ghats from Igatpuri (southwestern part of Nasik) to southern edge of the Deccan Traps, from Mahoney (1988). The approximate boundaries between formations are indicated by dashed lines. The name of each formation is shown. Stippled pattern at right presents Archean basement.

Table 3.1 The distinction criteria of (a) geological, petrographical and geochemical, (b) detailed geochemical, information in the allocation of samples to formations.

(a)

Formation boundary	Criteria for definding the formations
Desur-Panhara	chemical break (Sr, Ba, Zr/Nb)
Panhara-Mahabaleshwar	chemical break (TiO_2, Sr, Ba, Zr/Nb)
Mahabeleshwar-Ambenali	chemical break (Ba, Ba/Y, Zr/Nb, $^{87}Sr/^{86}Sr$)
Ambenali-Poladpur	concentrations of Ba
Poladpur-Bushe	chemical break (TiO_2, Sr, Zr/Nb, $^{87}Sr/^{86}Sr$)
Bushe-Khandala	chemical break (TiO_2, $^{87}Sr/^{86}Sr$)
Khandala-Bhimashankar	lava type (compound or simple flow) and existence of GPB (Giravali+Monkey Hill GPB)
Bhimashankar-Thakurvadi	existence of GPB (Manchar GPB) chemical break (MgO)
Thakurvadi-Neral	existence of GPB (Tunnel Five GPB)
Neral-Igatpuri	existence of GPB (Kashele GPB)
Igatpuri-Jawhar	existence of GPB (Thal Ghat GPB)

(b)

Formation	TiO_2 (wt. %)	Sr (ppm)	Ba (ppm)	Ba/Y	Zr/Nb	$^{87}Sr/^{86}Sr$ (initial ratio)
Desur	< 2.25	> 230	> 150		< 12.5	
Panhara	< 2.2	< 200	< 100		> 12.5	
Mahabeleshwar	> 2.0	> 225	> 80	> 4	< 13.0	> 0.705
Ambenali		< 290	< 100	< 3.5	9.0-16.5	< 0.705
Poladpur			> 100		> 11.0	0.705-0.713
Bushe	< 1.5	< 190			> 18.0	> 0.713
Khandala						< 0.713

(Beane *et al.*, 1986; Bodas *et al.*, 1988; Hooper *et al.*, 1988; Khadri *et al.*, 1988). These criteria for dividing each formation are also summarized in Table 3.1. For illustrating the example of geological criteria, it may be seen that the lava flows occurring beneath the lower than Bhimashankar Formation are essentially of compound type with only a few simple flows, while those of Khandala Formation of simple type. The interformational chemical variations for the lower six formation are scattered compared to those of upper six formations (for example, Ambenali basalts are chemically homogeneous). Each formation comprises several members having distinct petrographical and geochemical characteristics. The Jawhar, Igatpuri and Thakurvadi formations consist of nine, four and twenty-four members, respectively (Bodas *et al.*, 1988; Khadri *et al.*, 1988).

B. Central and Eastern area

Stratigraphy of Central and Eastern area of Deccan Traps have not been investigated in details, compared to that of Western Ghats area. The investigations in this region are essentially restricted to a few and far apart areas (Allmukhamedov and Zolotukhin, 1988; De, 1994; Sen and Cohen, 1994; Srivastava *et al.*, 1988; Subbarao *et al.*, 1994). Therefore, definite framework for this area is yet to be established.

2. Method of classification of stratigraphy

A. Data set

Fig. 3.2 shows the locations of the sections for which data are presented in this thesis. The region between Igatpuri (northernmost part) and Ambenali (southernmost part) is defined as Western Ghats area in this study. For the sake of descriptive convenience, the area falling between 74°30' and 77° longitudes (ST, EL, AJ, BU, CK,

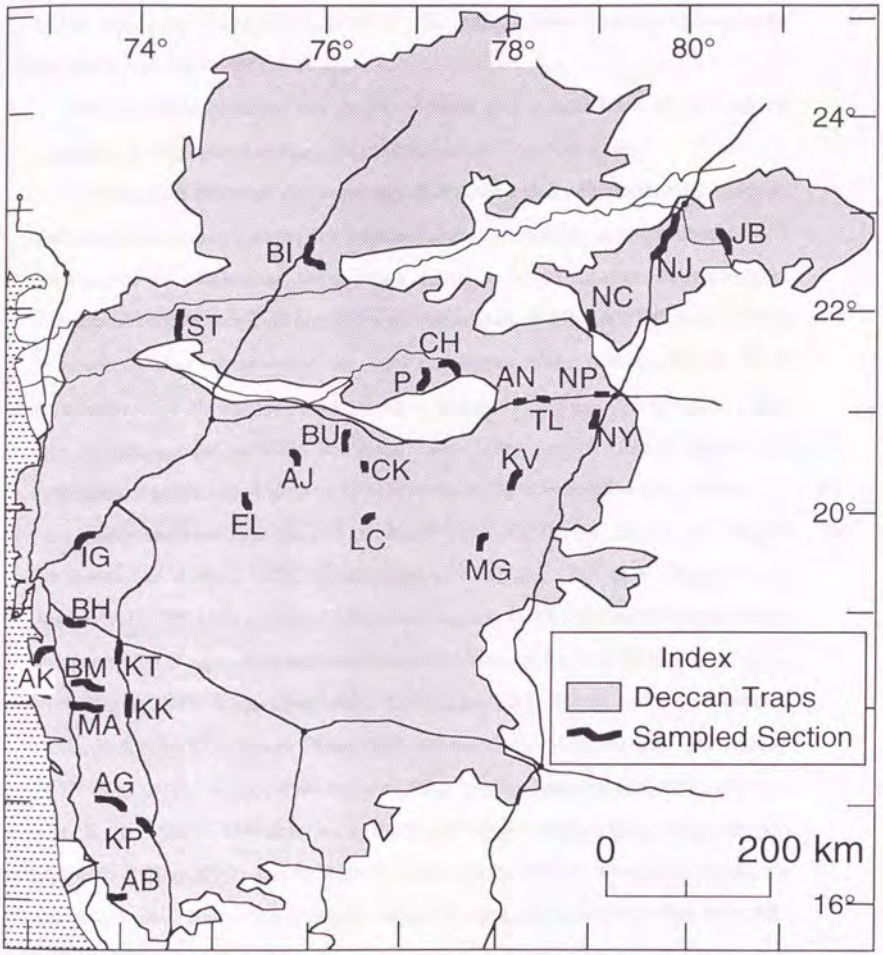

Fig. 3.2 Location map of sections used in this study. Abbreviation of each section is as follows; AB=Amboli, KP=Kolhapur, AG=Amba Ghat, MA=Mahabaleshwar, BM=Bhor-Mahad, KK=Khambatki, KT=Katraj, AK=Alibag-Khopoli, BH=Bor Ghat, IG=Igatpuri, ST=Shahada-Toranmal, EL=Ellora, BI=Barwaha-Indore, AJ=Ajanta, BU=Buldana, CK=Chikhali-Khamgaon, LC=Lonar Crater, P=Akot-Harisal, CH=Chikaldara, AN=Amravati-Nagpur, TL=Talegaon, MG=Mahur Ghats, KV=Kalalgaon-Vaghapur, NY=Bori, NP=Nagpur, NC=Nagpur-Chhindwara, NJ=Nagpur-Jabalpur, JB=Jabalpur-Mandla.

LC) is included in the central Deccan, while those sections which are located to the east of 77° (P, CH, AN, TL, MG, KV, NY, NP, NC, NC, JB) are considered to represent eastern area of Deccan (Fig. 3.2).

In this thesis, chemical stratigraphy of study area is established on the basis of geological, petrographical and geochemical characteristics of lava flows.

The Deccan Traps are predominantly tholeiitic basalts, with minor alkalic, felsic, and ultramafic intrusive rocks. The Deccan basalts are typically microporphyritic with phenocrysts of plagioclase, subordinate augite and rare olivine. Petrographical characteristics of Deccan Trap lava flows are summarized in Table A1. The modal degree of phenocrysts is variable and the most porphyritic rocks contain 30 vol. % of phenocrysts. The phenocrysts are set in a groundmass consisting of plagioclase, augite, rare olivine, opaque minerals and glass. Some lavas contain glomero-porphyritic aggregates of augite and plagioclase crystals occasionally in association with olivine.

Major and trace elements (Rb, Sr, Ba, Y, Zr, V, Cr, Ni, Cu, Zn, Ga, Nb, Sc, Th) for samples of Amboli (AB), Mahabaleshwar (MA), Bor Ghat (BH), Igatpuri (IG), Ajanta (AJ), Chikaldara (CH), Chikhali-Khamgaon (CK), Amravati-Nagpur (AN), Talegaon (TL), Nagpur (NP) sections were analyzed by Professor S. Aramaki, and those of Kolhapur (KP), Amba Ghat (AG), Khambatki (KK), Katraji (KT), Bhor-Mahad (BM), Buldana (BU), Lonar Crater (LC), Mahur Ghat (MG), Kalalgaon-Vaghapur (KV), Bori (NY), Nagpur-Chhindwara (NC), Nagpur-Jabalpur (NJ) and Jabalpur-Mandla (JB) sections were analyzed by Professor T. Fujii. Samples from Alibag-Khopoli (AK), Akot-Harisal (P) and Shahada-Toranmal (ST) sections were analyzed by the author including Rare-earth elements, Hf and Sc data of six sections (BM, MA, KK, BU, P, CH).

B. Analytical methods of major and trace elements

For the whole rock analysis, samples were crushed into cm-size pieces in iron mill. Xenocrysts were removed by hand-picking. Then samples were crushed into mm-size pieces and they were packed in agate ball mill and crushed into fine powder. For the analyses of major elements, 0.4000 ($\pm$0.009) g of dried rock powder was mixed with $Li_2B_4O_7$ flux with a ratio of 1 : 10. This mixture was put into a $Pt_{95}Au_5$ crucible and was melted to form a glass bead by a microwave oven. For the analysis of trace elements, about 4.0 g dried rock powder was pressed into a disc held in a 7.0 g boric acid container.

Major and Trace element analyses were carried out with the Rigaku System 3080ES XRF of the Earthquake Research Institute, University of Tokyo. Whole rock compositions analyzed by XRF are presented in Table A2 a.

The non-destructive instrumental neutron activation analysis (INAA) was used for the determination of trace elements and some major elements. They are Fe, K, Na as major elements and rare-earth elements (La, Ce, Nd, Sm, Eu, Tb, Yb and Lu), Sr, Ba, Zr, Th, U, Hf, Ta, Sc, Co and Cr as trace elements.

For the analyses, about 80 mg rock powder was sealed in the quartz capsule and was activated with thermal neutrons for one hour with 5.5×10^3 n/cm^{2}s at S pipe in the JRR-4 reactor of Japan Atomic Energy Research Institute. JB-1, JR-2 and BCR3 (standard rocks of Geological Survey of Japan) were also activated as standard and for cross-checking among them. After a suitable cooling time, gamma-ray spectra of activated samples were counted with both XTRA-type and LEG-type Ge (Li) detector coupled to the 2048 and 4096 multi-channel analyzers at the Faculty of Sciences, Gakushuin University.

The measurements were made three times for each sample. First, after three days cooling, the samples were counted for one hour to determine mainly Na_2O and K_2O. Second, after one week cooling, the samples were counted again for two hours to determine mainly La, Nd, Sm, U, Lu, Yb, Ba and Sc. Third, after one month cooling, the samples were counted again for seven- ten hours to determine mainly Fe, Ce, Eu, Tb,

Sr, Th, Hf, Ta, Zr and Co. The dead time was restricted to less than 20 % (mainly 10-18 %).

The abundance of each element was obtained in comparison with that of one of standard references. When plural values for one element were calculated, the elemental abundance was determined to be the average value of them or the selected value obtained from the best precision peak. Accuracy of the analyses has been checked by comparison of the results for rock reference samples such as JB-1, JR-2 and BCR3 (Imai *et al.*, 1995). Analytical error for rare-earth elements is less than ±10%. Whole rock compositions of seven samples determined by INAA are listed in Table A2 b.

C. Method of classification

a. Western Ghats area

In this study, data from ten sections have been used to determine the stratigraphy of the Western Ghats area (Fig. 3.3). As described earlier, chemical stratigraphy for the Western Ghats has been established by previous workers (Beane *et al.*, 1986; Bodas *et al.*, 1988; Cox and Hawkesworth, 1984, 1985; Devey and Lightfoot, 1986; Khadri *et al.*, 1988; Lightfoot *et al.*, 1990; Mahoney *et al.*, 1982, Mitchell and Cox, 1988; Mitchell and Widdowson, 1991). Therefore, for recognizing the stratigraphic divisions in Western Ghats, I used the geological, petrological and geochemical classification based largely on criteria established by Beane *et al.* (1986), Cox and Hawkesworth (1984, 1985), Devey and Lightfoot (1986), Lightfoot *et al.* (1990) as described in Table 3.1.

Within the upper six formations (younger than Bushe Formation), each one can be separated from the other on the basis of major changes in the geochemistry. These changes are easily recognizable in the plots of certain geochemical parameters against height for each section (Figs. 3.4 a-j).

The lower six formations (older than Thakurvadi Formation) are distinguished separately mainly on the basis of megascopic and field observations such as the existence

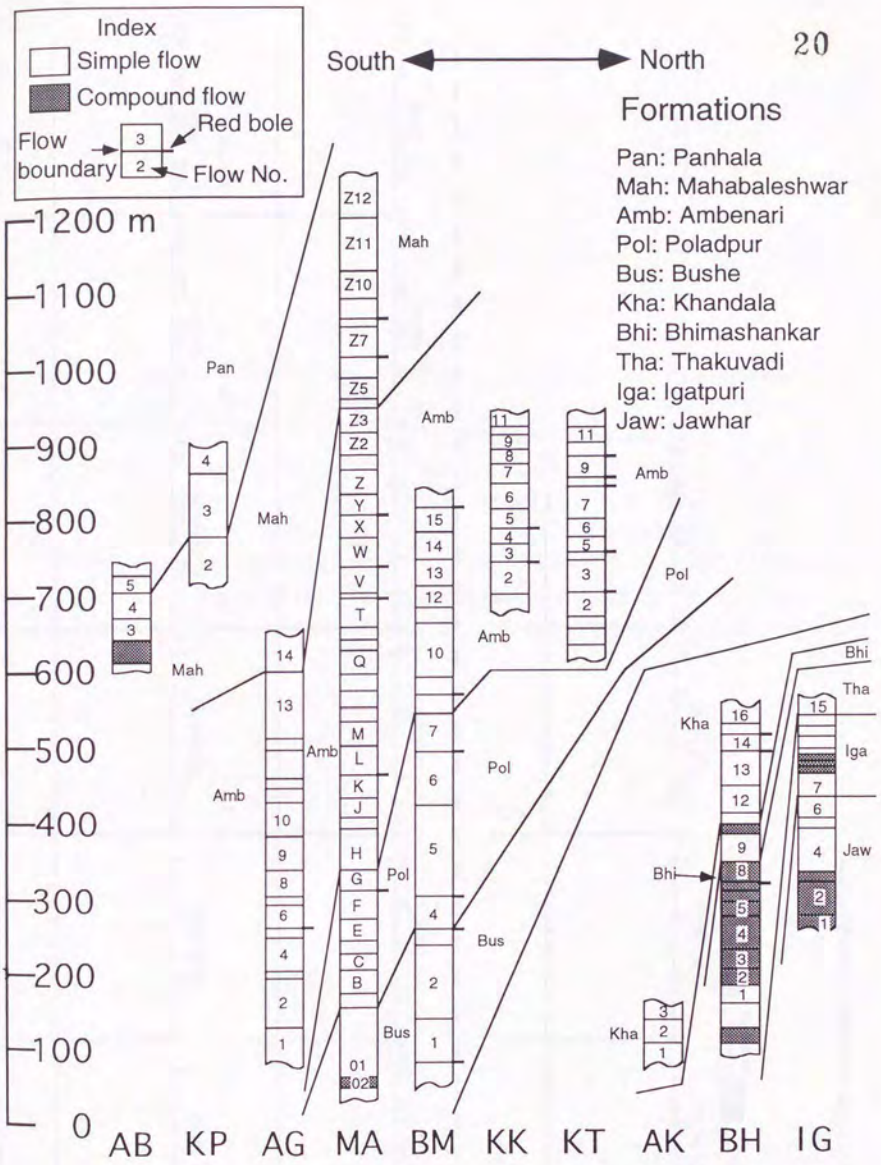

Fig. 3.3 Section showing the flow correlation along the Western Ghats area between Igatpuri and Amboli. Abbreviation for each section is the same as Fig. 3.2. The approximate boundaries between formations are indicated by solid lines. Formation names, flow numbers, flow boundaries and red bole beds are shown.

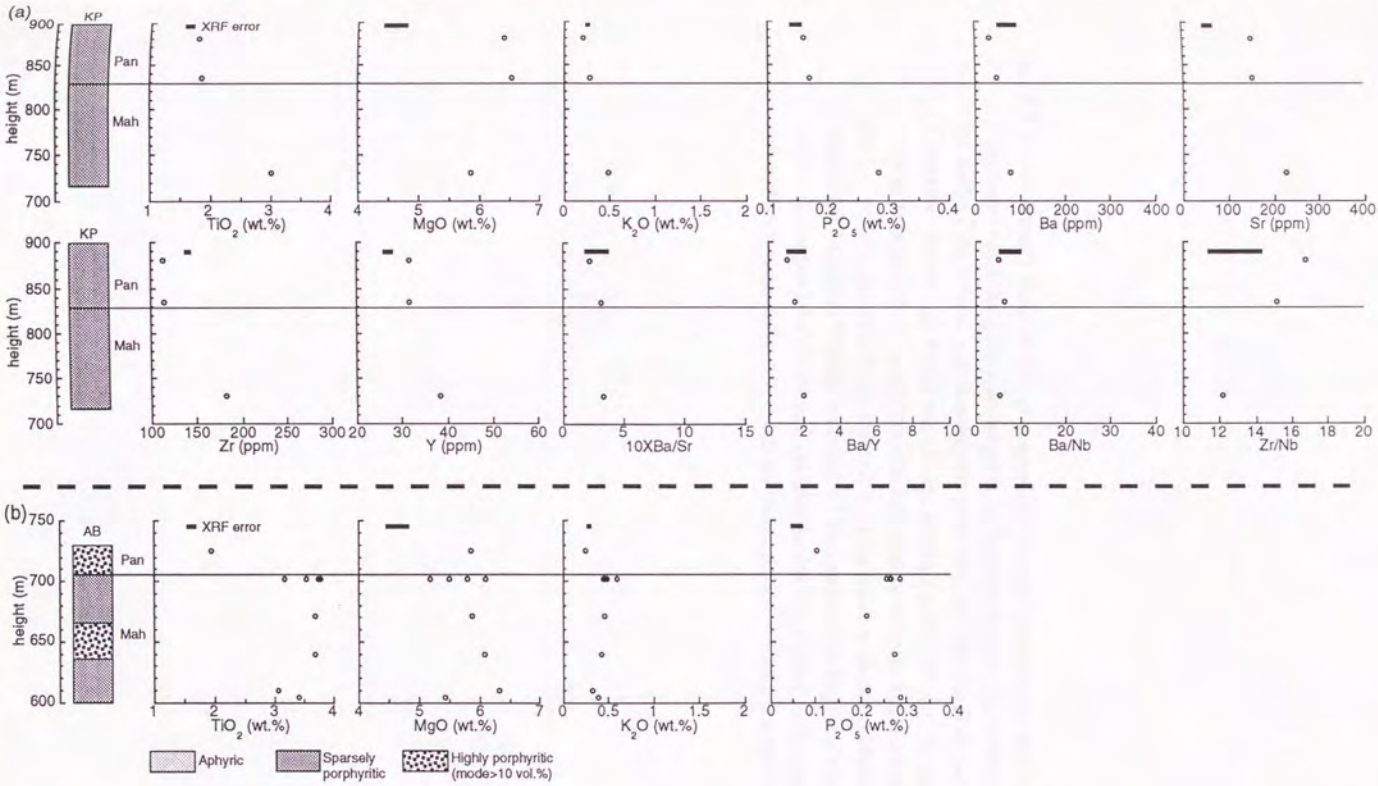

Fig. 3.4 (See next page for explanation)

Fig. 3.4 (--- continued) Plots of modal proportions of total phenocrysts and chemical compositions against stratigraphic height in (a) Kolhapur section, (b) Amboli section, (c) Amba Ghat section, (d) Mahabaleshwar section, (e) Bhor-Mahad section, (f) Khambatki section, (g) Katraj section, (h) Alibag-Khopoli section, (i) Bor Ghat section, (j) Igatpuri section, (k) Shahada-Toranmal section, (l) Ajanta section, (m) Buldana section, (n) Akot-Harisal section, (o) Chikaldara section, (p) Mahur Ghats section, (q) Kalalgaon-Vaghapur section, (r) Bori section, (s) Nagpur-Chhindwara section, (t) Nagpur-Jabalpur section, (u) Jabalpur-Mandla section. Abbreviation for each section is same as Fig. 3.2. Group names are shown. MK means marker flow.

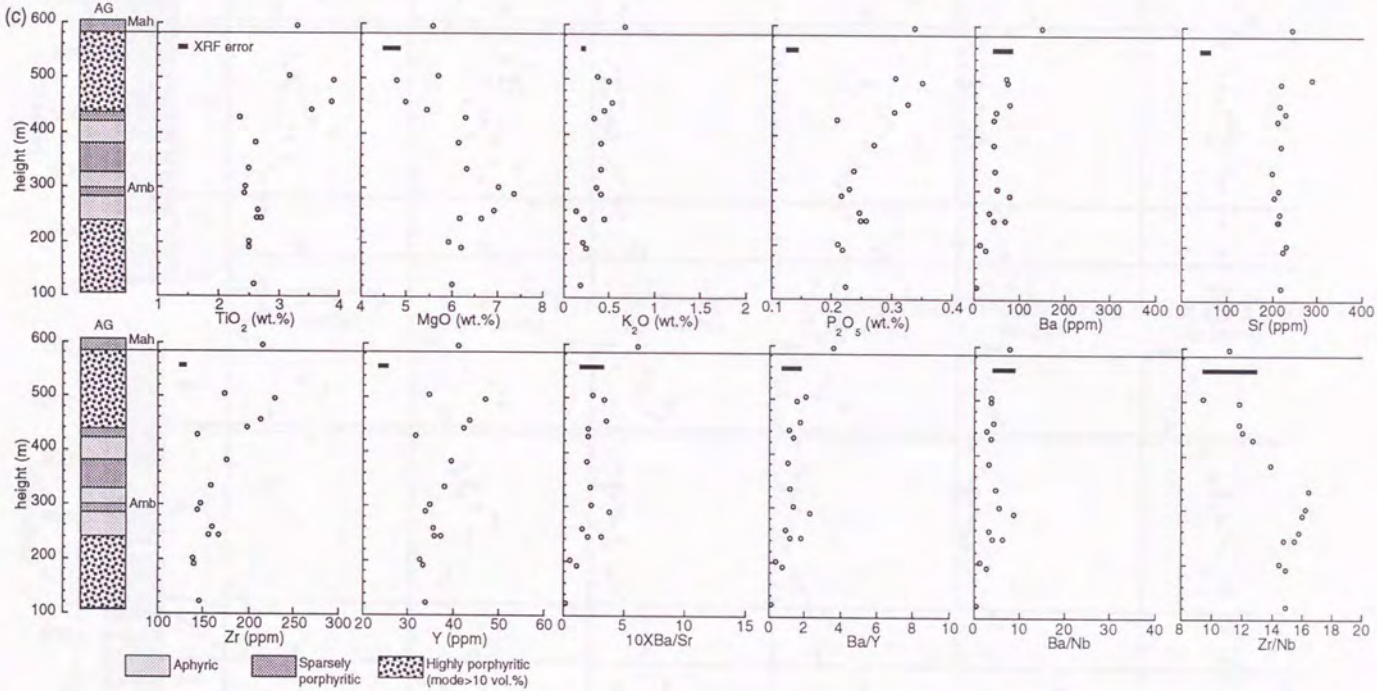

Fig. 3.4 (--- continued)

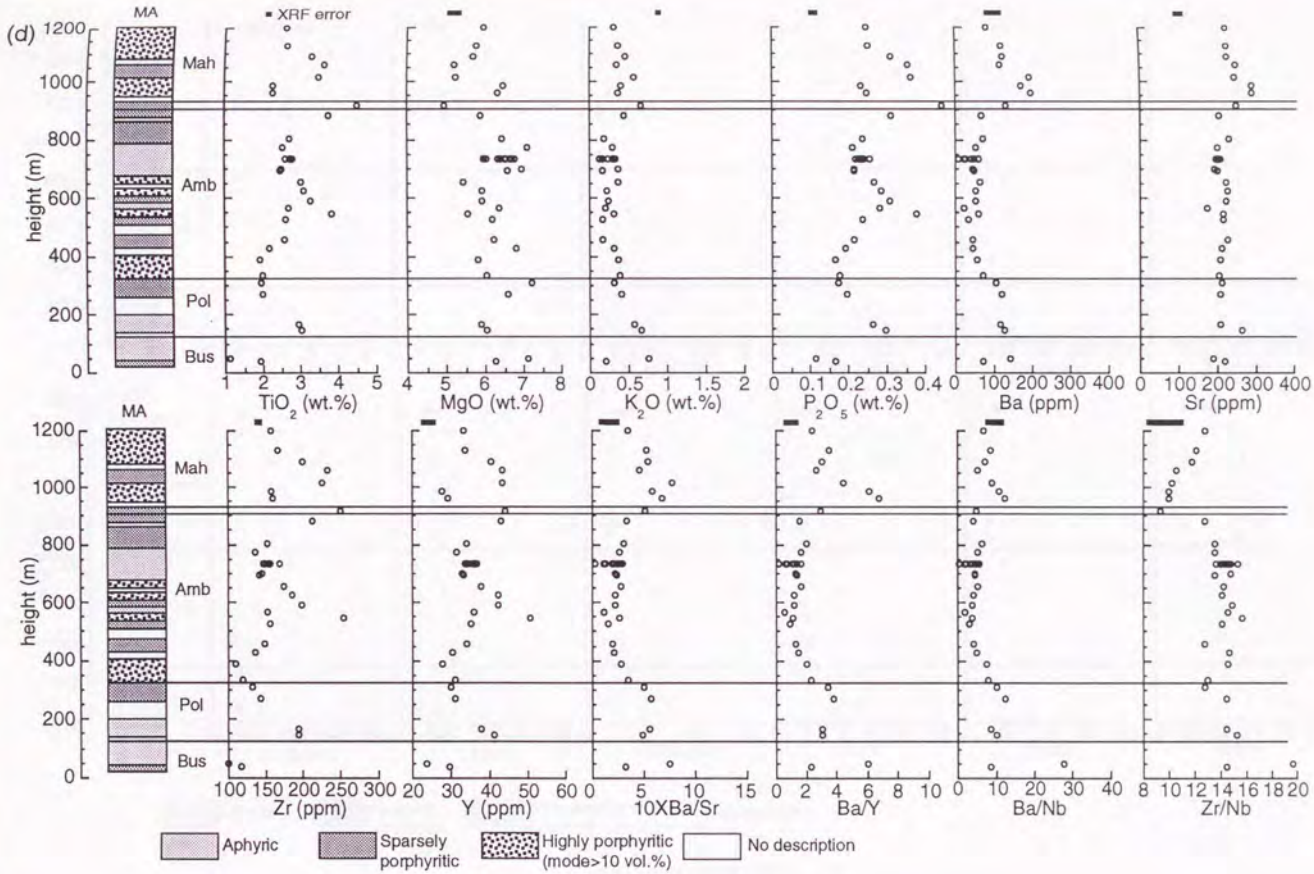

Fig. 3.4 (--- continued)

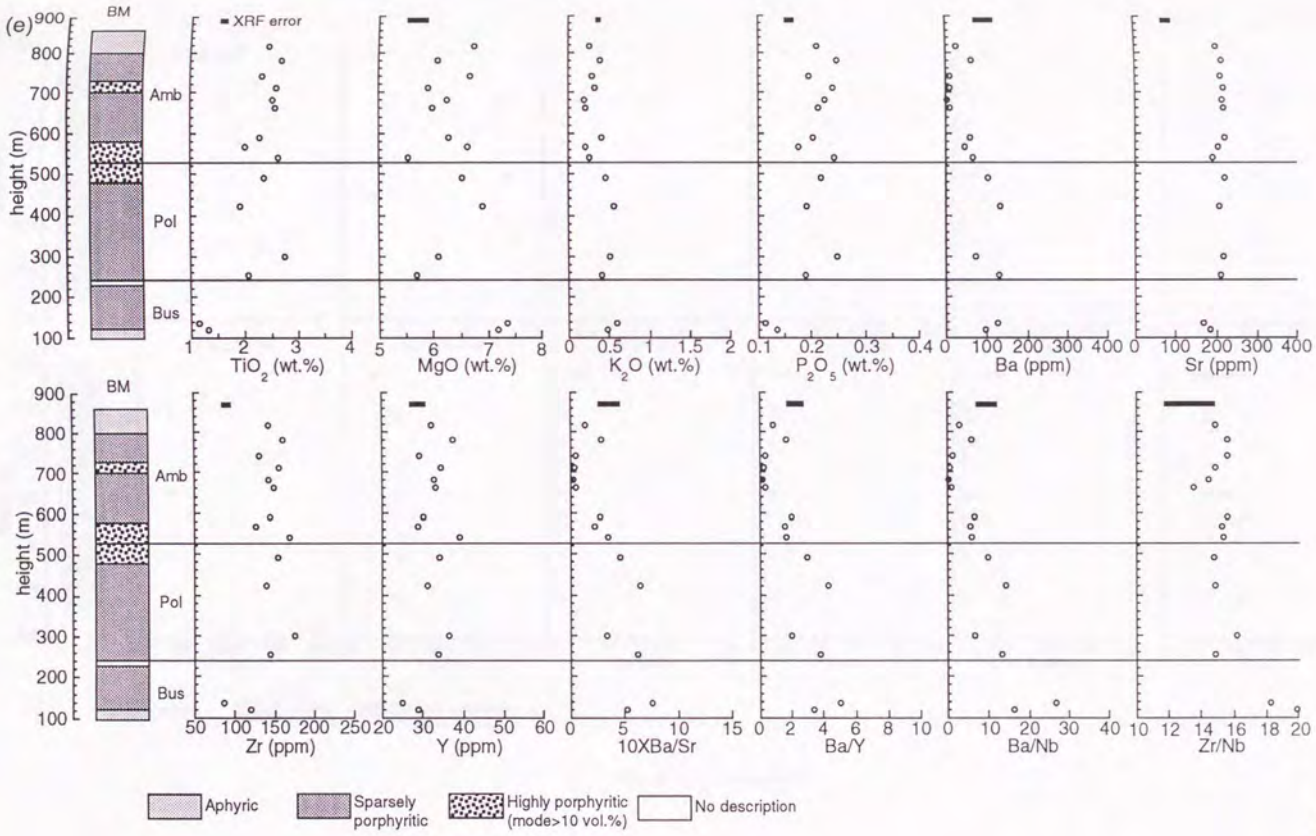

Fig. 3.4 (--- continued)

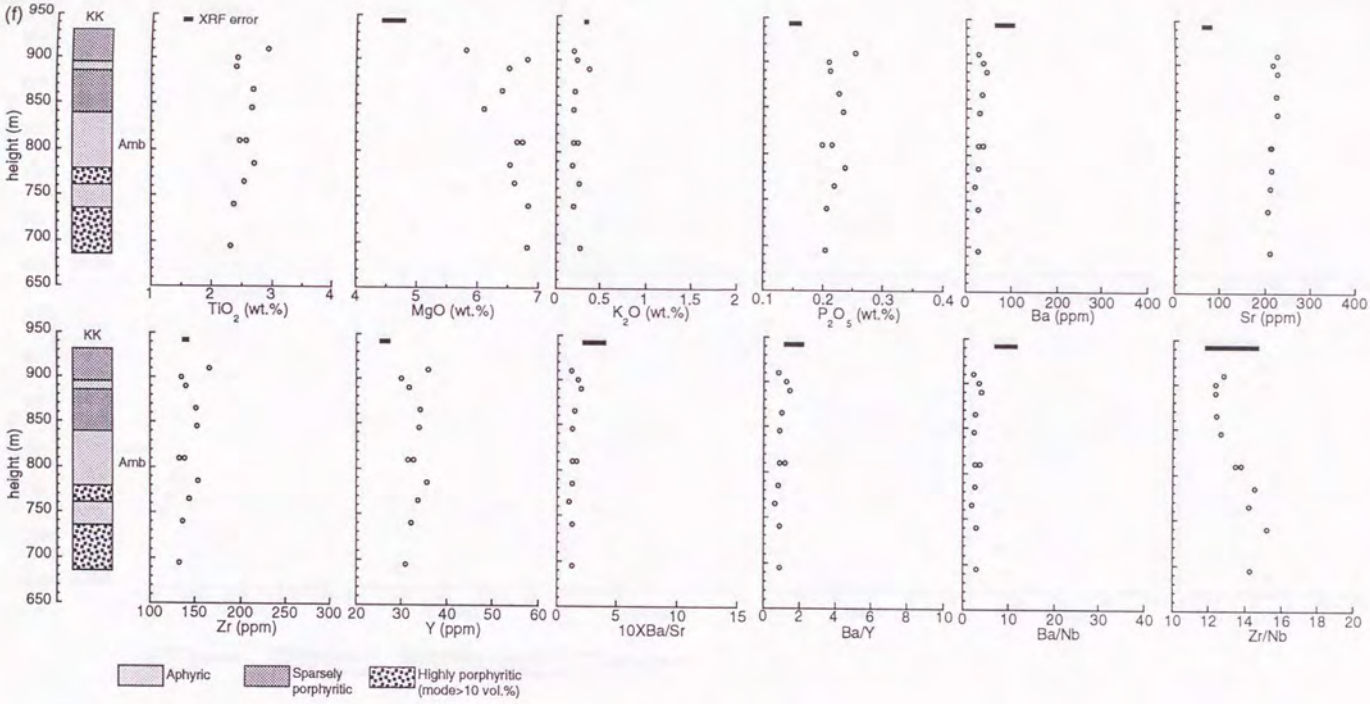

Fig. 3.4 (--- continued)

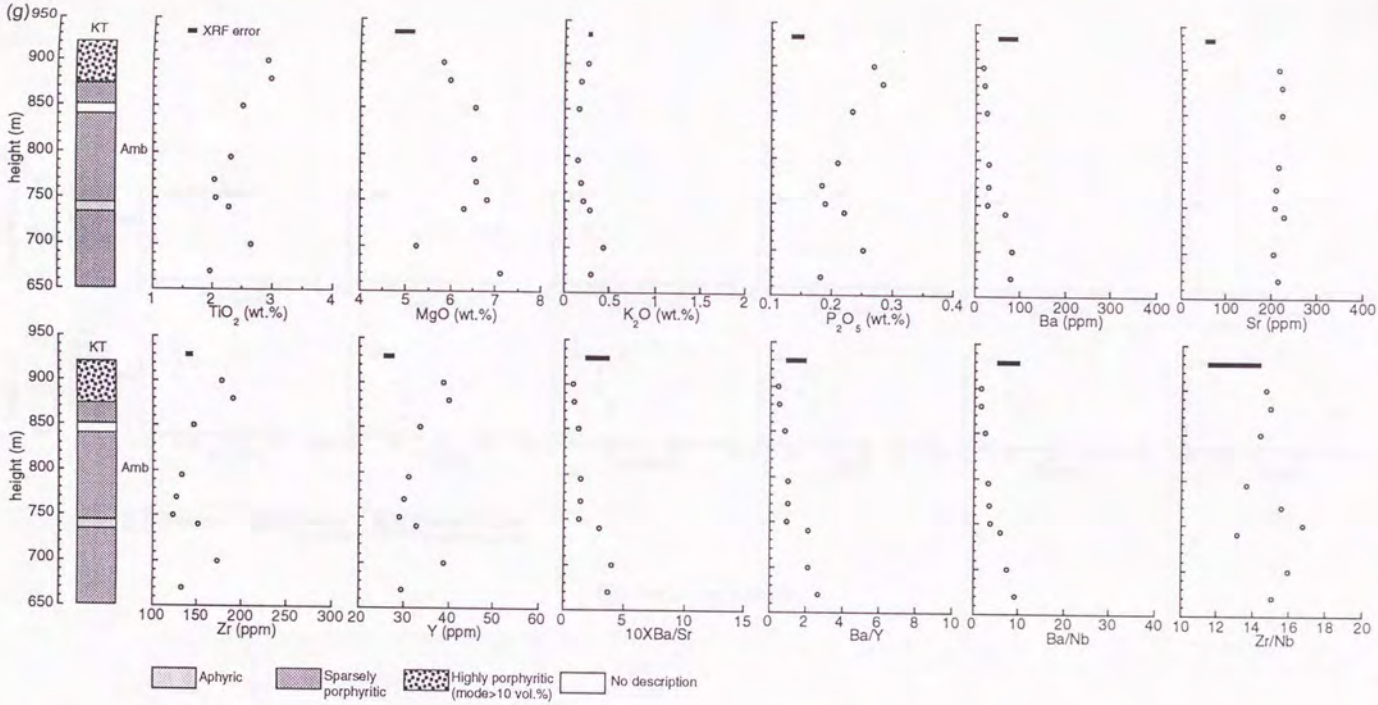

Fig. 3.4 (--- continued)

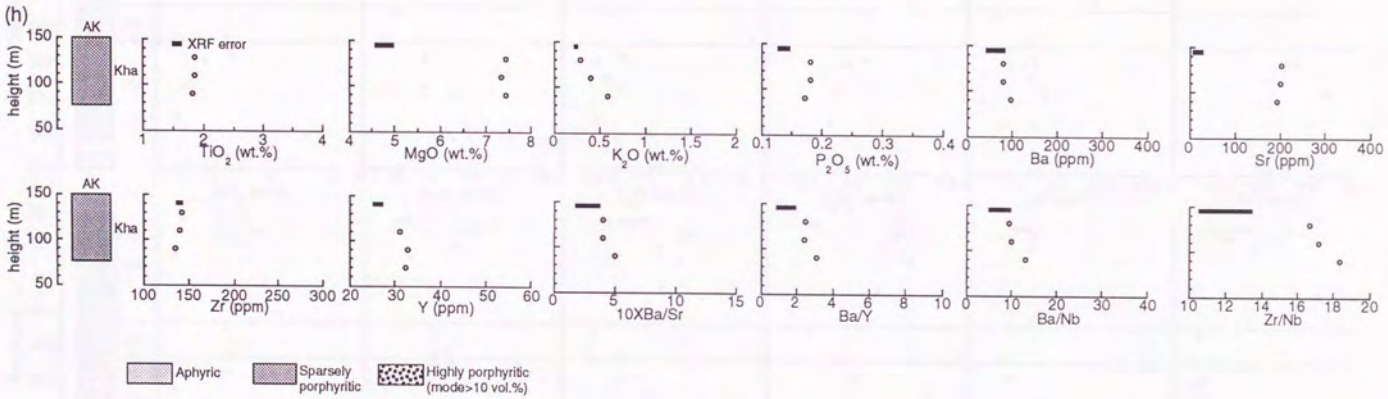

Fig. 3.4 (--- continued)

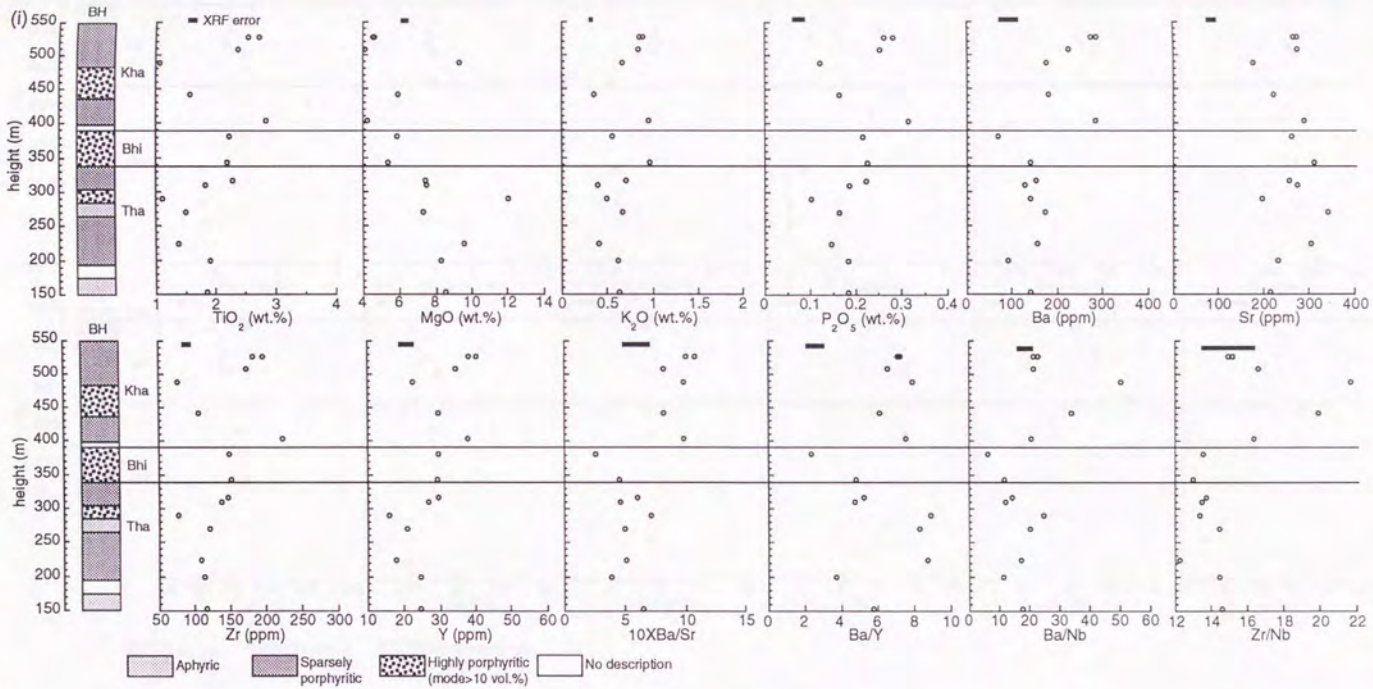

Fig. 3.4 (--- continued)

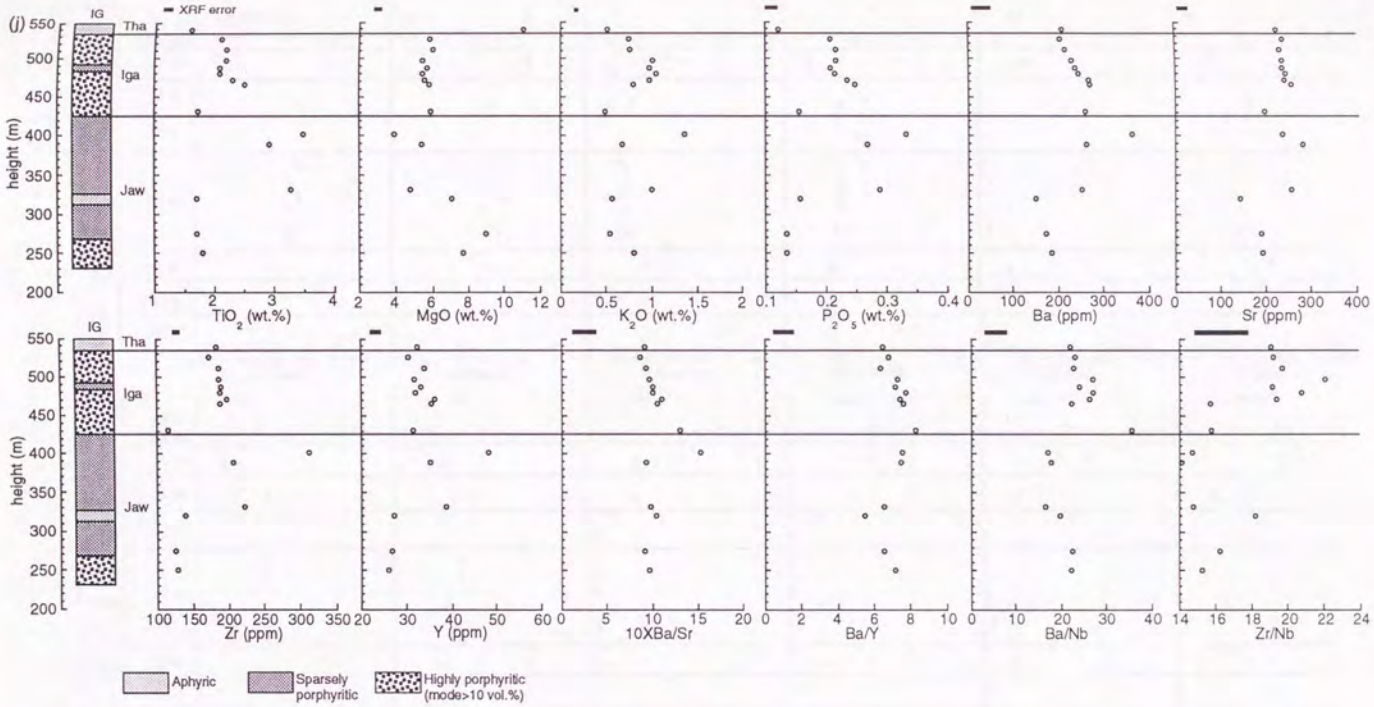

Fig. 3.4 (--- continued)

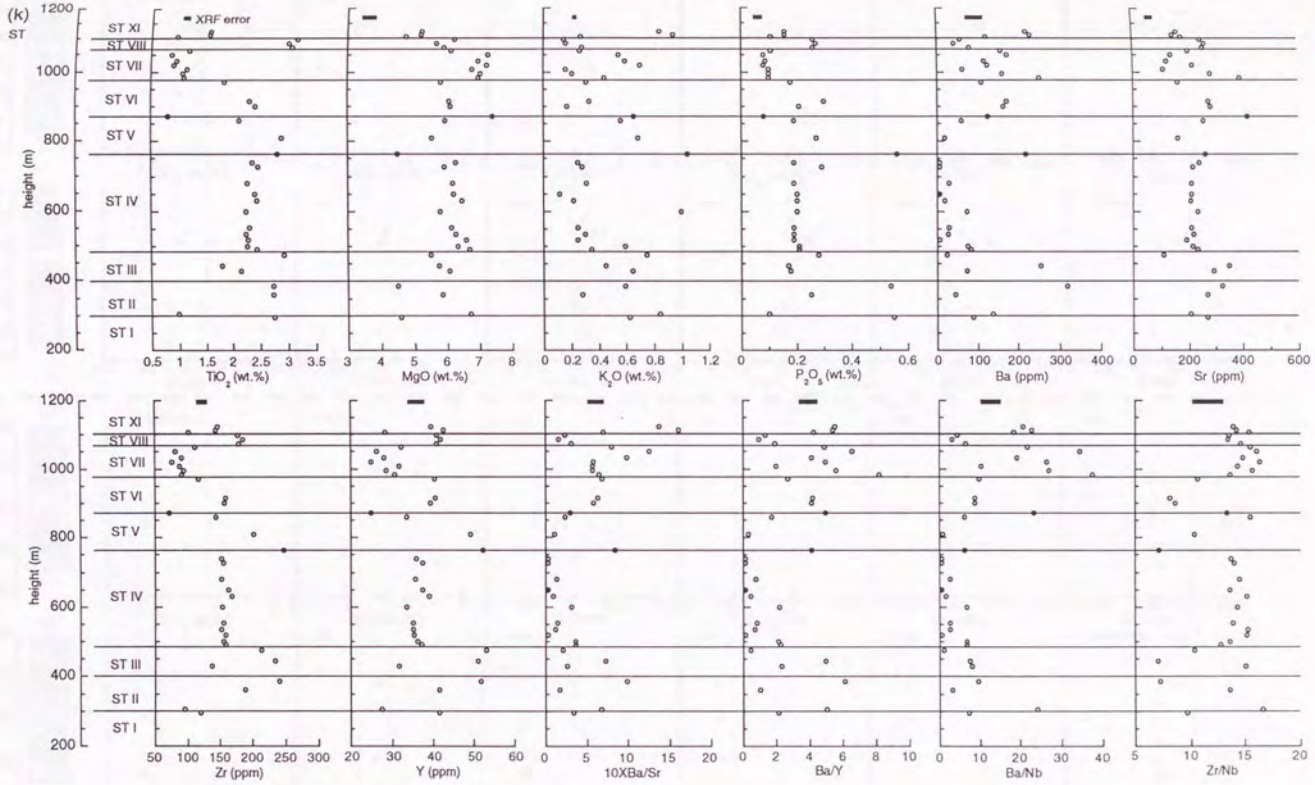

Fig. 3.4 (--- continued)

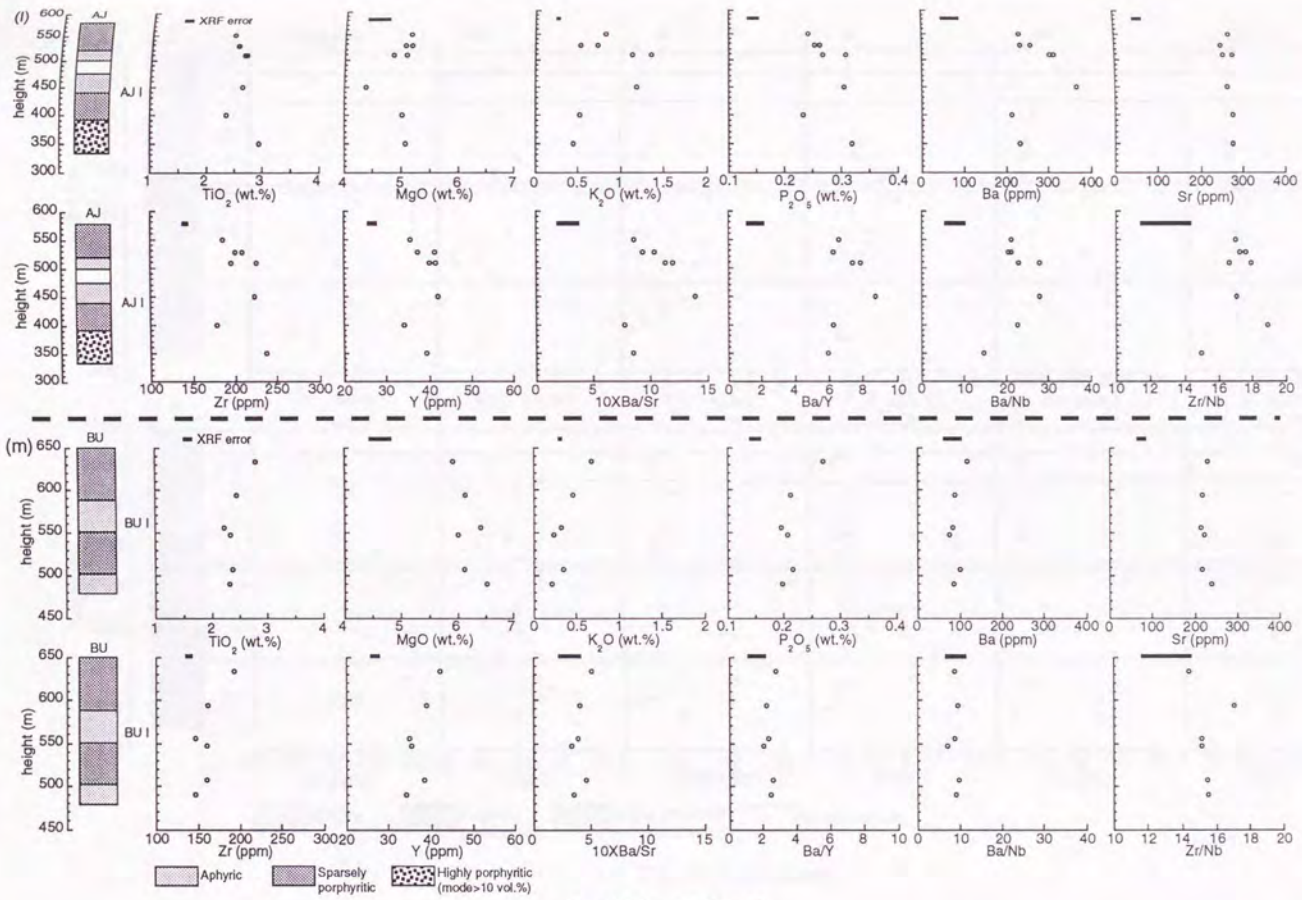

Fig. 3.4 (--- continued)

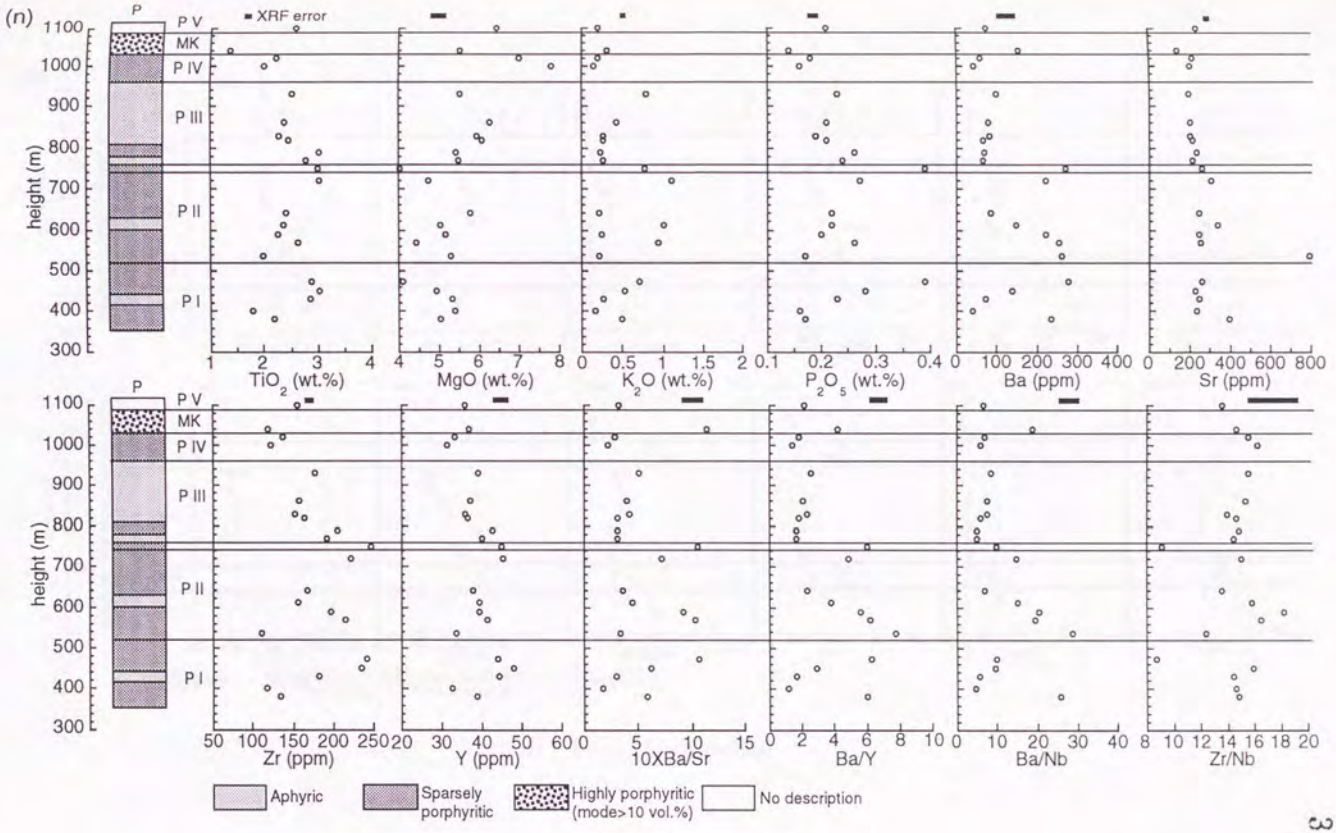

Fig. 3.4 (--- continued)

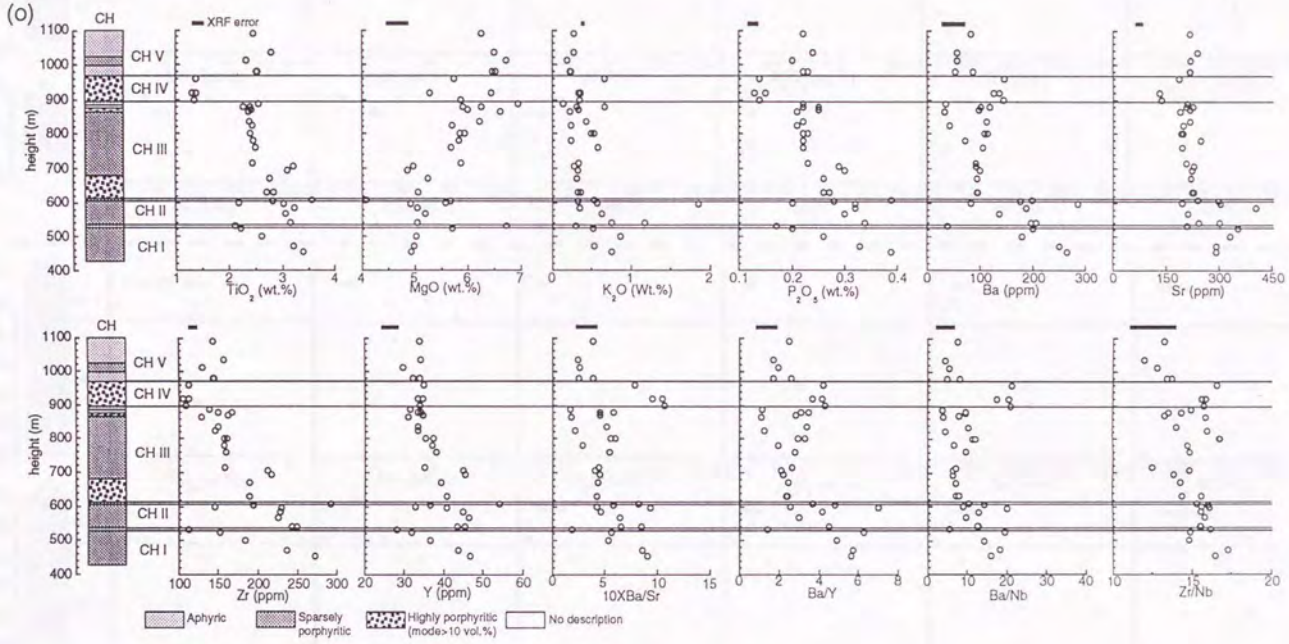

Fig. 3.4 (---continued)

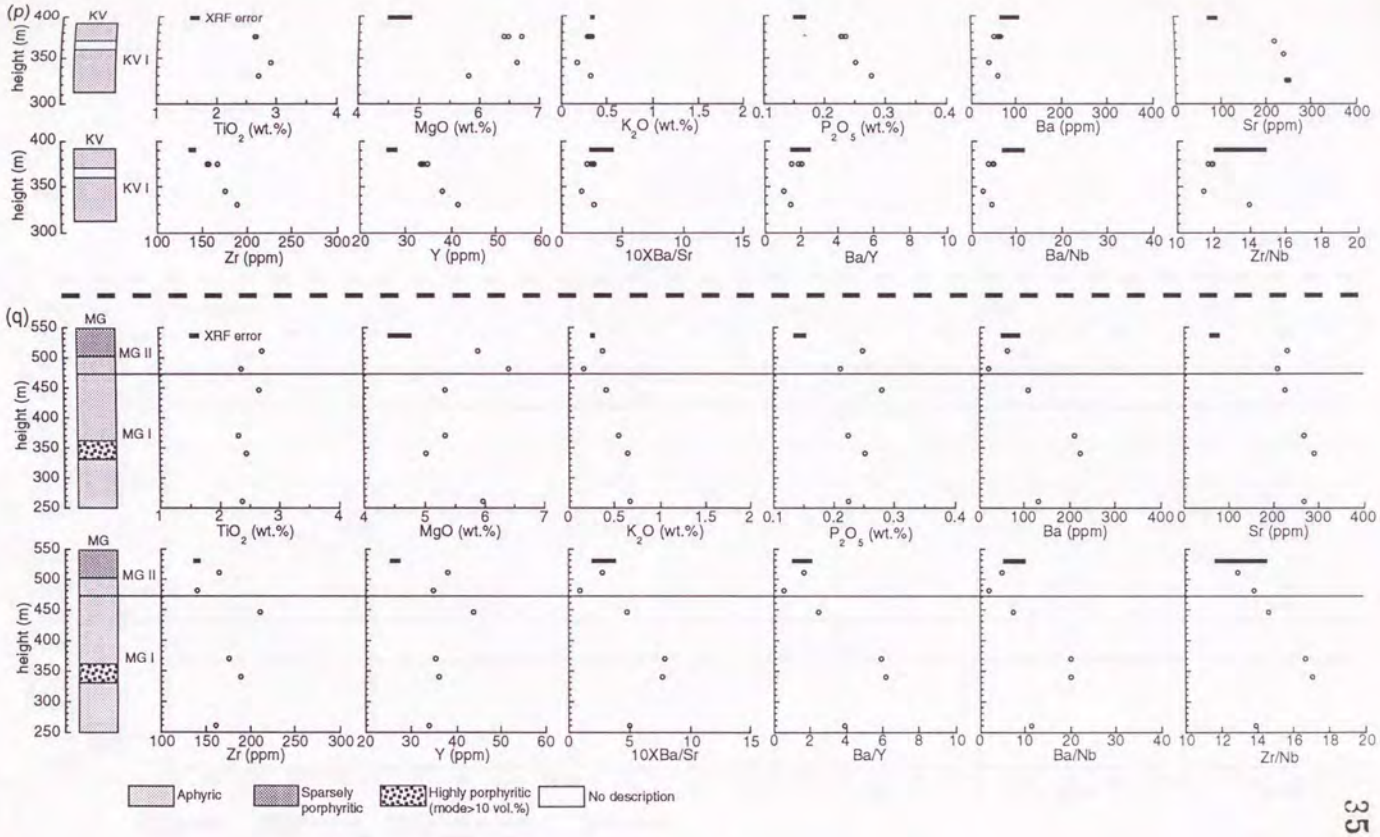

Fig. 3.4 (---continued)

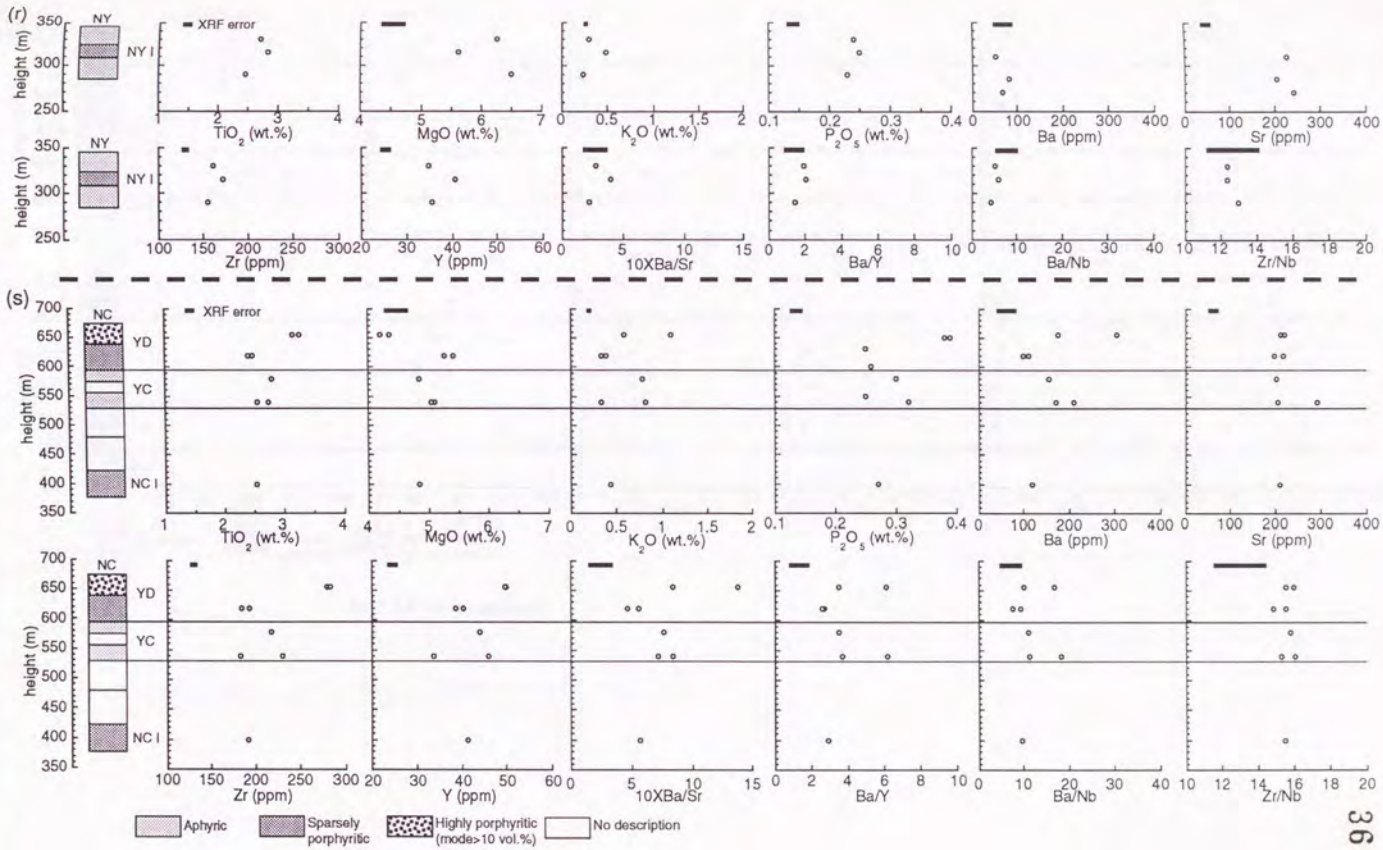

Fig. 3.4 (--- continued)

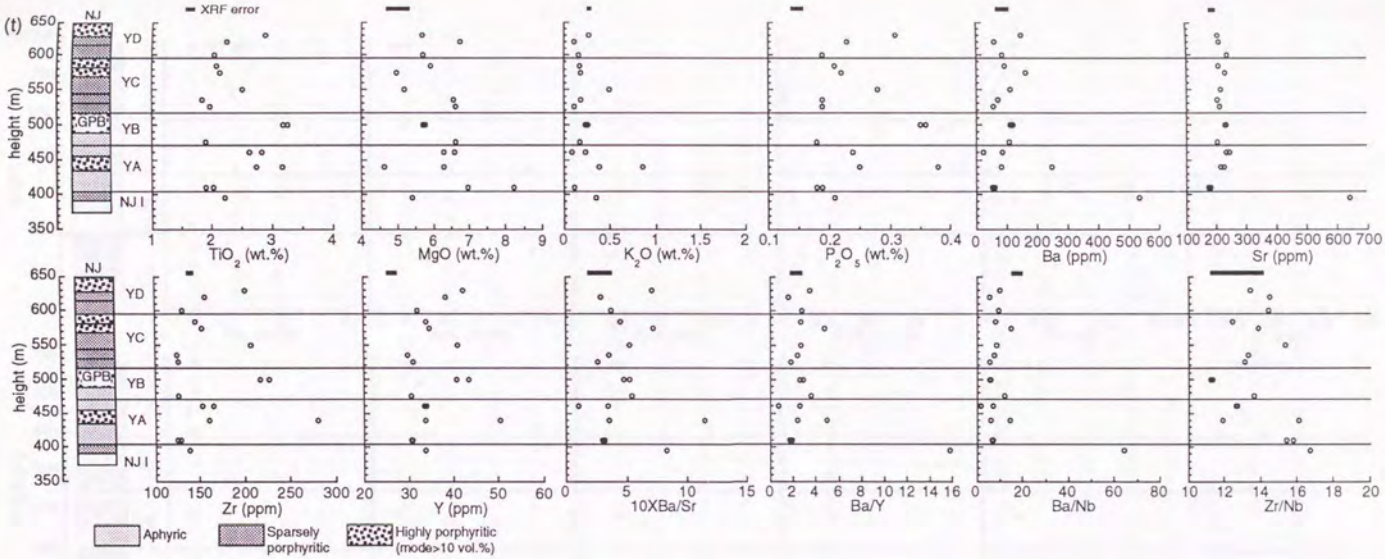

Fig. 3.4 (--- continued)

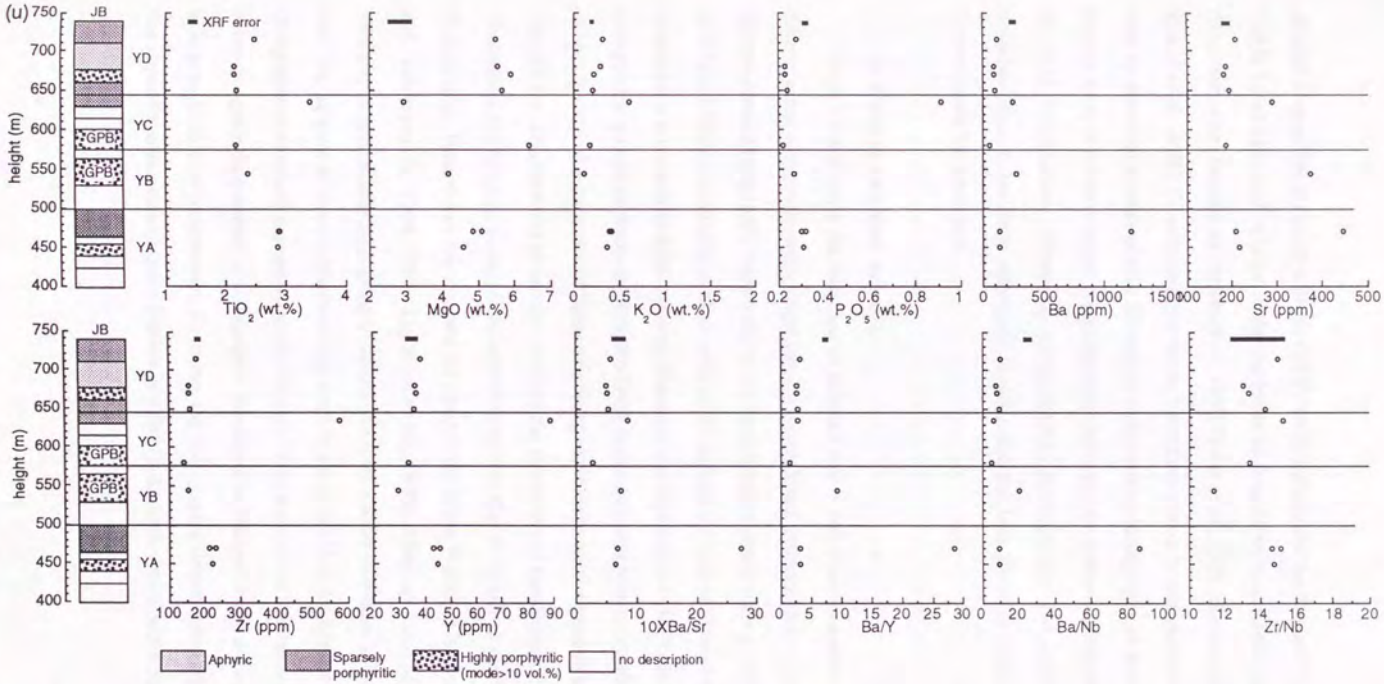

Fig. 3.4 (---continued)

of giant plagioclase phenocryst basalt (GPB) horizon at or near the formation boundary (Table 3.1 a). Chemical variation within the lower six formations is scattered compared to those with upper formations (Beane *et al.*, 1986; Bodas *et al.*, 1988; Hooper *et al.*, 1988; Khadri *et al.*, 1988). Consequently, lower six formations cannot be separately recognized only by chemical characteristics. Therefore, in this study, stratigraphy of the lower six formations is of tentative nature compared to that of upper six formations because of lack of field information. However, using mainly microscopic and geochemical characteristics, it has been attempted to designate the lava flows to the respective formations on the lower part.

b. Central and East area

Figs 3.4 k-u show the variation in selected major and trace elements and inter element ratios with stratigraphic height for samples collected from sections in Central and Eastern Areas. Stratigraphic framework for the central and eastern parts is yet to be firmly established. Hence, continuity of all or some of the formations from west into central and eastern parts is not known with certainty. Therefore, the lava pile is divided into different stratigraphic groups on the basis of marked shift in the chemical parameters observed at or near the top of a sequence of flows exhibiting similar chemical signature as seen in Figs 3.4 k-u. The chemical parameters used are the abundance of certain major and trace elements or the ratios of incompatible elements such as Ba, Sr, Y and so on. Table 3.1 shows comprehensive key criteria used for recognizing in the Western Ghats area (Cox and Hawkesworth, 1984, 1985; Lightfoot *et al.*, 1990). They are used to find out similarity of each stratigraphic group in central and eastern areas with those in the western part. The purpose of this correlation at this stage is not to establish the continuity of the stratigraphic formations recognized in the Western Ghats into central and eastern sectors, but to recognize the presence of stratigraphic formations in this part which are chemically analogous to those of western part. Therefore, the stratigraphic classification proposed in this paper for central and eastern Deccan is a tentative nature which will need further

refinement and confirmation by backing up detailed field and geochemical studies in closely spaced sections.

c. Probable late-stage alteration, and flow heterogeneity

There is a possibility of the effect of the alteration and flow heterogeneity on Deccan Trap basalts. Cox and Hawkesworth (1985) reported the results of possible element mobility within a single flow on the basis of samples collected on different scale; the largest (collected at intervals of 100 m from a simple flow), the intermediate (intervals of 10 m) and the smallest (opposite ends of a simple hand- specimen) scale. They showed excellent reproducibility in most analytical values for each sample. Therefore, they concluded that chemical difference generated by the alteration is negligibly small than the interformational chemical variations.

To clarify the interflow heterogeneity, I also analyzed major and trace elements of ten samples collected from a 35 m thick-simple flow (MA-W flow) in Mahabaleshwar section (Fig. 3.2). Mode of phenocrysts (plagioclase and augite) in these rocks is variable between 0 to 5 vol.% (Table A1) and degree of alternation is also variable. In contrast, the chemical variation is negligible which shows the interflow heterogeneity in respect of major and trace elements (Table 3.2). However, this variation is conspicuously smaller than the variation within the Ambenali Formation (the most homogeneous formation on the Deccan Traps) which includes flow MA-W.

3. Regional stratigraphy

A. Western Ghats area

Chemical stratigraphy established in this study is largely consistent with previous works. Previous workers (*e.g.*, Beane *et al.*, 1986; Devey and Lightfoot, 1986) reported that thickness of each formation between Mahabaleshwar and Bhimashankar is largely

Table 3.2 Whole rock compositions of basalts collected from a MA-W flow. All analyses by XRF. FeO*: total iron as FeO.

Sample No.	SiO2 (wt.%)	TiO2	Al2O3	FeO*	MnO	MgO	CaO	Na2O	K2O	P2O5
MA-W-21	48.16	2.83	13.91	14.83	0.20	6.78	10.95	2.00	0.13	0.22
MA-W-22	48.70	2.79	13.75	14.90	0.20	6.02	11.10	2.15	0.17	0.23
MA-W-23	48.93	2.77	13.60	14.30	0.21	6.42	11.18	2.23	0.13	0.23
MA-W-24	49.24	2.81	13.37	14.65	0.22	6.35	10.61	2.20	0.34	0.23
MA-W-25	48.90	2.77	13.38	14.62	0.21	6.69	10.67	2.19	0.33	0.24
MA-W-26	48.83	2.75	13.52	14.52	0.21	6.65	10.72	2.26	0.31	0.23
MA-W-27	48.96	2.78	13.31	14.56	0.20	6.54	10.86	2.26	0.29	0.24
MA-W-29	49.19	2.64	13.36	14.88	0.19	5.98	10.98	2.29	0.24	0.25
MA-W-31	48.84	2.79	13.33	14.66	0.22	6.57	10.89	2.22	0.24	0.23
MA-W-51	48.81	2.80	13.39	14.60	0.21	6.67	10.71	2.24	0.34	0.23
average	48.86	2.77	13.49	14.65	0.21	6.47	10.87	2.20	0.25	0.23
1-sigma	0.29	0.05	0.20	0.18	0.01	0.28	0.19	0.08	0.09	0.01
XRF error	0.15	0.01	0.18	0.03	0.01	0.05	0.03	0.04	0.01	0.01

Sample No.	Rb (ppm)	Sr	Ba	Y	Zr	V	Cr	Ni	Nb	Th
MA-W-21	0.4	196	22	34	155	464	122	94	11	1.9
MA-W-22	6.2	206	6	36	154	405	121	83	11	2.6
MA-W-23	1.7	208	25	34	152	396	124	90	11	0.8
MA-W-24	3.1	203	49	36	152	363	113	84	11	4.0
MA-W-25	3.7	195	48	34	148	373	120	82	10	1.8
MA-W-26	2.9	208	58	36	149	393	117	87	10	1.9
MA-W-27	3.5	204	61	36	155	437	120	85	11	2.1
MA-W-29	10.6	203	40	37	169	398	124	81	12	0.2
MA-W-31	4.7	199	40	34	148	423	129	86	11	1.8
MA-W-51	4.9	198	46	34	147	394	124	85	10	0.3
average	4.2	202	39	35	153	404	121	86	11	1.7
1-sigma	3	5	17	1	7	30	4	4.0	0.7	1.1
XRF error	3	11	18	2	6	10	13	3.3	1.1	2.2

Sample No.	Ba/Y (ratio)	Zr/Nb	Ba/Nb	Ba/Sr X10	TiO2/Y X100
MA-W-21	0.63	14.4	1.99	1.10	8.21
MA-W-22	0.16	14.1	0.53	0.28	7.69
MA-W-23	0.75	14.4	2.38	1.21	8.21
MA-W-24	1.35	13.7	4.37	2.39	7.80
MA-W-25	1.41	14.8	4.75	2.44	8.22
MA-W-26	1.62	14.6	5.69	2.79	7.71
MA-W-27	1.69	14.5	5.67	2.98	7.73
MA-W-29	1.09	14.0	3.31	1.98	7.16
MA-W-31	1.18	14.0	3.81	2.01	8.23
MA-W-51	1.35	15.3	4.82	2.34	8.13
average	1.12	14.4	3.73	1.95	7.91
1-sigma	0.48	0.5	1.68	0.84	0.35
XRF error	0.52	1.6	1.72	0.90	0.47

constant over the Western Ghats area. Further, they showed that the formation boundaries have southerly dips. These characteristics can be also seen in Fig. 3.3.

Geological, petrographical and geochemical characteristics for each formation are described below in descending order.

Desur Formation (Des)

Desur Formation is regarded as youngest in the Western Ghats area. In course of this study, however, no samples belonging to this formation were collected. Thickness of this formation is more than 100 m at the margin of the Deccan Traps (Devey and Lightfoot, 1986; Lightfoot *et al.*, 1990).

The boundary between the Desur and underlying Panhala formation is defined by change in chemical characters (Devey and Lightfoot, 1986; Lightfoot *et al.*, 1990). Basalts in Desur Formation have larger Rb, Sr, Ba abundance and lower Zr/Nb ratios than those of underlying Panhala Formation.

Panhala Formation (Pan)

Panhala Formation can be seen only in the southernmost part of the Western Ghats area (AB and KP sections in Figs. 3.3, 3.4 a, b). Thickness of this formation is more than 120 m at Kolhapur (Figs. 3.3, 3.4 a). In thin sections rocks are sparsely to highly porphyritic basalts. Phenocrysts are plagioclase, subordinate augite in Amboli section, whereas they are plagioclase, subordinate olivine and rare augite in Kolhapur section (Table A1). This formation is characterized by lower abundance of TiO_2 (< 2.0 wt.%), Rb (< 4 ppm), Ba (< 50 ppm) and Sr (< 160 ppm) and higher Zr/Nb (>15) ratios compared to underlying Mahabaleshwar Formation (Figs. 3.4 a, b).

Mahabaleshwar Formation (Mah)

This formation can be distinguished from the underlying Ambenali formation by the sharp break in the chemical characters at the formation boundary. It is seen that the flows in the lower part of the Mahabaleshwar formation have larger Ba abundance and higher

Ba/Y and lower Zr/Nb ratios than those of Ambenali Formation. This formation boundary can be seen in the Amba Ghat and Mahabaleshwar sections (Figs. 3.4 c, d). In Mahabaleshwar section, the flow MA-Z3 which occurs at the formation boundary has transitional chemical characters from Mahabaleshwar to Ambenali. Therefore, this lava flow does not belong to any of these formations but is defined as a boundary flow. All flows of this formation comprise sparsely to highly porphyritic basalts whose phenocryst content varies from 1 to 20 vol.% (Table A1). Nearly 50 % of the flows contain plagioclase as the only phenocryst phase, while the remaining flows have plagioclase and subordinate or rare olivine and augite as phenocrysts.

Lightfoot *et al.* (1990) pointed out differences in chemical composition within lavas of Mahabaleshwar formation as indicated by the conspicuously higher contents of TiO_2 and Zr in flows near Kolhapur than those in flows of type Mahabaleshwar section. Therefore, they proposed that these flows may be referred to as the Kolhapur unit of Mahabaleshwar Formation. In this study, all Mahabaleshwar basalts of Kolhapur, Amboli and Amba Ghat sections and three successive flows (from MA-Z7 to MA-Z10) in the Mahabaleshwar section have composition similar to the Kolhapur unit (*e.g.*, $TiO_2 >$ 3.0 wt.%, Zr > 180 ppm in Table A2) proposed by Lightfoot et al. (1990) and as such they are considered to represent the Kolhapur unit of Mahabaleshwar Formation.

Ambenali Formation (Amb)

Ambenali Formation is more than 500 m thick and comprises a sequence of chemically homogeneous basalt flows. Thickness of this formation is > 472 m in Amba Ghat section, 581 m at Mahabaleshwar section, > 276 m in Bhor-Mahad section, > 216 m in Khambatki section and 231 m in Katraj section (Figs. 3.4 c, d, e, f, g). It consists of more than 20 simple lava flows in Mahabaleshwar section (Fig. 3.4 d).

It was noted that there is no sharp break in any chemical characters between the Ambenali and Poladpur formation, and in all cases this boundary is transitional. Cox and Hawkesworth (1984, 1985) defined the boundary between Ambenali and Poladpur based on the Ba content (Table 3.1 b; Ambenali < 100 ppm).

Ambenali flows vary from aphyric to highly porphyritic with some containing 30 vol.% of phenocrysts. Plagioclase phenocrysts are accompanied by subordinate amount of augite phenocrysts or phenocrysts of both augite and olivine.

Chemical compositions of Ambenali basalts are characterized by very low K_2O (most rocks < 0.4 wt.%), Rb (most rocks < 10 ppm) and Ba (< 100 ppm) abundance, and low Ba/Y (most rocks < 2.0) ratios (Table A2 a). Ambenali basalts have distinctive isotopic signature within the Deccan marked by uniform and low $^{87}Sr/^{86}Sr$ ratios (Cox and Hawkesworth, 1985; Lightfoot and Hawkesworth, 1988; Lightfoot *et al.*, 1990; Mahoney *et al.*, 1982; Peng *et al.*, 1994).

Poladpur Formation (Pol)

This formation is distinguished from the underlying Bushe formation by sharp chemical break. The rocks of this formation have higher TiO_2, P_2O_5, Sr, Zr abundance and lower Zr/Nb ratios than those of the Bushe Formation (Figs. 3.4 d, e). Chemically the flows exhibit mixed characters transitional from underlying Bushe to overlying Ambenali formation. Further, chemical composition of the basalt flows within the formation also exhibits continuous change from the base to top (Figs. 3.4 d, e)

The lava flows of Poladpur Formation are of simple type, whereas those in Bushe Formation are amygdaloidal compound flows. Consequently, the boundary between Bushe and Poladpur Formation can also be traced on the basis of differences in physical characters of lava flows. All formations younger than Poladpur are mainly composed of simple flows. Poladpur Formation consists of seven and four simple flows at Mahabaleshwar and Bhor-Mahad sections, respectively (Figs. 3.4 d, e). Thickness of this formation is 189 m at Mahabaleshwar section and 287 m at Bhor-Mahad section.

The rocks of this formation are mainly aphyric to sparsely porphyritic basalts (phenocryst contents are 0-12 vol.%). Phenocrysts are mainly of plagioclase with subordinate augite and minor olivine (Table A1).

Cox and Hawkesworth (1985) subdivided the Poladpur Formation into Lower and Upper Poladpur on the basis of sudden increase in TiO_2, Zr concentrations and $^{87}Sr/^{86}Sr$

ratios in the sequence corresponded to mark the base of upper Poladpur Formation. However, this chemical break has not been recognized in course of the subsequent rock by Devey and Lightfoot (1986), Lightfoot *et al.*, (1990). Therefore, the distinction between Lower and Upper Poladpur has been eliminated in this study.

Bushe Formation (Bus)

Bushe Formation is characterized by a distinctive chemical composition. The top lava flows have low TiO_2, Zr, Sr abundance and high SiO_2, MgO, Rb abundance compared with lava flows of most of the younger formations (Figs. 3.4 d, e). The most distinctive feature is, however, the high Zr/Nb ratios (> 18 ppm). The $^{87}Sr/^{86}Sr$ ratios of Bushe basalts are also conspicuously higher (> 0.713) than those of other formations.

The Bushe flows are nearly aphyric basalts with plagioclase phenocryst content ranging from 0 to 7 vol.% (Table A1). It essentially consists of compound flows. Chemical composition of MA-001 flow of Mahabaleshwar section is similar to Ambenali or Poladpur basalts (Fig. 3.4 d), however, this belongs to Bushe formation because of its compound nature and the composition of the overlying MA-002 flow is of typical Bushe type.

Khandala Formation (Kha)

The basalt flows of Khandala Formation are characterized by high TiO_2 and Ba abundances compared to those in the overlying Bushe Formation (Beane *et al.*, 1986). Further, the lava flows in this formation are dominantly of simple type. Therefore, this formation can be easily differentiated from the overlying Bushe and underlying Bhimashankar Formations, which are mainly composed of the compound flows. In the Bor Ghat section, the upper five flows are of simple character which overlie the compound flow of Bhimashankar Formation (Fig. 3.3). Thickness of this formation is >123 m in Bor Ghat section (Fig. 3.4 i). Chemical composition of Khandala Formation varies widely (for example, MgO abundance ranges from 4.3 to 9.3 wt.%). The flows comprise sparsely to highly porphyritic basalts with phenocryst of plagioclase and olivine

and rare augite. The most MgO-rich basalt (BH-14) in this formation contains olivine phenocrysts only (Table A1).

The flows of Alibag-Khopoli section are chemically homogeneous. (Fig. 3.4 h) However, these compositions are different from upper six formations (*e.g.*, Ba < 100 ppm, Zr/Nb > 16.5). Moreover, their petrographic characters, (composed of olivine and augite phenocrysts and plagioclase phenocrysts are absent. Table A1) are also different from that of upper six formations. Therefore, these lava flows belong to lower formations, possibly representing Khandala Formation, being essentially composed of simple lava flows (Fig. 3.3).

Bhimashankar Formation (Bhi)

Beane *et al.* (1986) defined that Bhimashankar Formation overlies the Mancher GPB and in turn is capped by the Giravali GPB and Monkey Hill GPB (Table 3.1), and comprises mainly of compound flows. In this study Bhimashankar Formation appears to be present in the middle part of Bor Ghat section (from 343 to 403 m above sea level in Fig. 3.4 i). The basal lava flow of this formation can be identified by its chemical composition exhibiting sharp decrease in MgO from > 7 wt.% to < 6 wt.% (Fig. 3.4 i). This character has also been emphasized by the Beane *et al.* (1986).

Rocks of Bhimashankar are highly porphyritic (12 vol.% of phenocrysts) with phenocrysts of dominant plagioclase and subordinate olivine.

Thakurvadi Formation (Tha)

This formation has been divided into lower, middle and upper parts based mainly on petrographic characters (Khadri *et al.*, 1988). These three groups contain six, eleven and seven members, respectively. The top of this formation is represented by the Manchar GPB which separates it from the overlying Bhimashankar formation (Table 3.1 a). Most rocks in this formation have high MgO contents (> 7.0 wt.%) of up to 12 wt.% (Beane *et al.*, 1986; Khadri *et al.*, 1988). Rocks of Thakurvadi formation can be

identified by this chemical character (Beane *et al.*, 1986). The uppermost lava flow at Igatpuri section may have belonged to Thakurvadi Formation (Fig. 3.4 j).

Thakurvadi Formation mainly comprises compound flows (Fig. 3.3) which are aphyric to highly porphyritic (> 40 vol.%). Some rocks contain glomeroporphyritic aggregates of augite phenocrysts. Phenocrystic assemblage in some flows is represented by augite or plagioclase phenocrysts only, while in others some phenocrysts of olivine and augite or plagioclase are noticed (Table A1)

Neral Formation (Ner)

This formation occurs situated between the underlying Kashele GPB and overlying Tunnel Five GPB. The Neral basalts have distinctive petrographic character, being rich in olivine and augite phenocrysts and devoid of plagioclase phenocrysts (Beane *et al.*, 1986). In case of the present work area containing flows of Neral Formation were not examined.

Igatpuri Formation (Iga)

The uppermost flow of this formation is defined as the Kashele GPB (Table 3.1). Bodas *et al.* (1988) recognized four members in this formation on the basis of petrographic and geochemical characteristics. The lava flows in the basal part of Igatpuri Formation contain higher MgO and CaO, and lower TiO_2, $P2O_5$, Zr, Y and Nb concentrations as compared with the uppermost lava flow of Jawhar Formation (Table 3.1). Following these criteria, the formation boundary is situated between IG-06 and IG-07 flows in Igatpuri section (Fig. 3.4 j).

Igatpuri formation is composed of both compound and simple flows (Fig. 3.3). Thickness of this formation is 109 m at Igatpuri section. Most rocks of Igatpuri formation are highly porphyritic (up to 25 vol.%) with phenocrysts of plagioclase, olivine and augite (Table A1).

Jawhar Formation (Jaw)

This constitutes the lowest formation in the Western Ghats and has been subdivided into nine members based mainly on textual characters and phenocryst assemblages of rocks (Bodas *et al.*, 1988). Beane *et al.* (1986) indicated that the top of the Jawhar Formation is represented by the Thal GPB layer (Table 3.1). In this study, this formation comprises basal six flows of Igatpuri section. The lower three are compound flows, whereas the upper three are of simple type. Thickness of this formation is more than 180 m in Igatpuri section. The lowest flow (IG-01) is highly porphyritic basalts. Phenocrysts are dominant plagioclase and subordinate augite. In comparison, upper five lava flows are mostly aphyric basalts (Table A1).

B. Central and Eastern area

Regional stratigraphic framework for western Deccan, based on geological and geochemical studies, is well established. However, as stated earlier, stratigraphy for central and eastern areas has not been established as yet. Based on the geological and geochemical study of basalt flows exposed in several sections located across the central and eastern Deccan, an attempt has been made to divide the lava pile into different stratigraphic groups. Further, it has also been attempted to correlate these groups with those of the western Deccan. It is pertinent to point out that this correlation is not attempted with the intentions of establishing the continuity of formations from west to east and is restricted to recognizing the presence of chemically analogous lavas piles in the central and eastern parts. More detailed studies in closely spaced sections will be necessary to establish the physical continuity of stratigraphic formations from west to east.

The stratigraphy of the Central and eastern area discussed in this chapter has been presented by Deshmukh *et al.* (1996a). A probable regional stratigraphic model, as

devised from present studies, for central and eastern areas is discussed at the end of this chapter and is shown in Fig. 3.5.

Shahada-Toranmal section (ST)

This is one of the thickest section in the central part of Deccan Traps and contains 41 flows within 835 m thick lava pile. Detailed discussion on the stratigraphy of this section will be presented by Nair *et al.* (1996). The lava flows exhibit wide chemical variations and it is possible to group the flows showing similar chemical signature into 9 different stratigraphic units on the basis of vertical variation in chemical parameters (Fig. 3.4 k).

Group I (ST I) comprises flow 1 only. Chemical composition of this flow shows typical Ambenali signature, however overlying sequence has similarity with the formations of the Western Ghats older than Ambenali.

Group II (ST II) comprises flows from 2 to 4. They exhibit mixed chemical signature of both Poladpur and Mahabaleshwar compositions. However, the upper groups have a typical Ambenali composition, hence these flows cannot be considered to be belonging to Mahabaleshwar and as such appear to represent transitional types of Poladpur and Ambenali compositions.

Group III (ST III) comprises three flows from 5 to 7. It can be seen that MgO content of this group increases with time. However, chemical characters differ to varying degrees. Flow 5 shows Ambenali composition, while 6 has similarity with Poladpur. Flow 7 is depleted in Ba and Sr and is enriched in Y and Zr. It compares with Ambenali in its Ba content and Zr/Nb and Ba/Y ratios, however, it has very low Sr content (109 ppm) compared to Ambenali. In view of these characters the flows represent a transitional sequence from Poladpur to Ambenali.

Group IV (ST IV) comprises 12 flows from 8 to 19 within 275 m thick lava pile. Their compositions are uniform and show typical Ambenali affinity except for flow 13 (ST-22 sample) which has high K_2O (0.99 wt.%) content (Fig. 3.4 k).

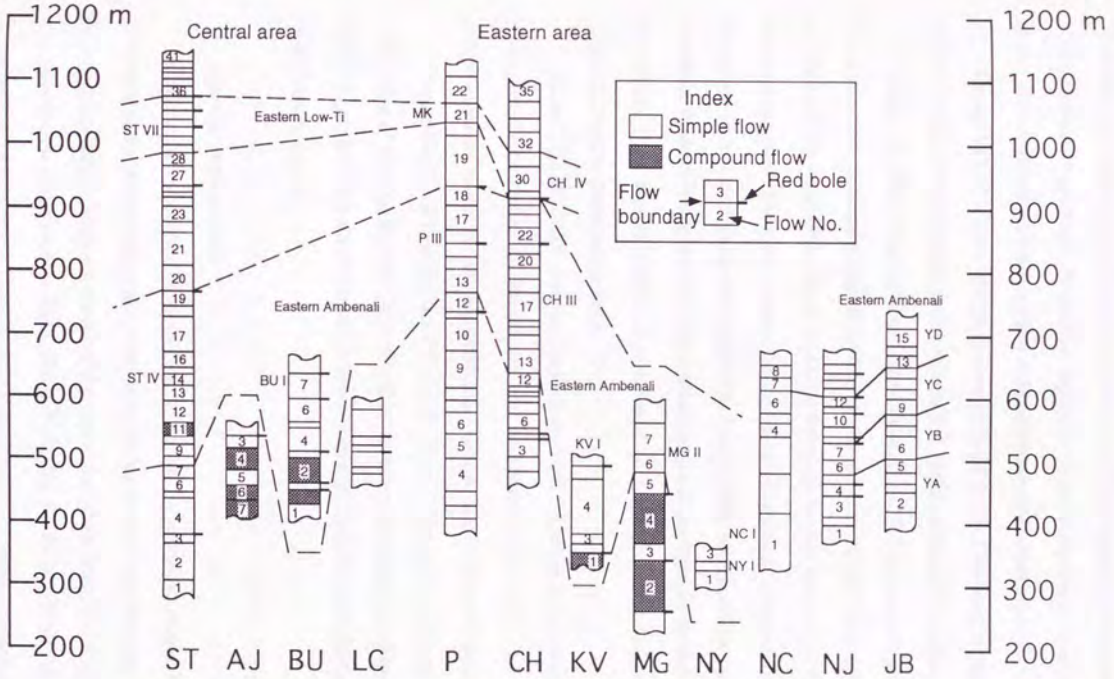

Fig. 3.5 Sections showing the relative locations of sampled profiles through the Deccan Traps along the Central and Eastern area between Shahada-Toranmal in the west and Jabalpur-Mandla in the east. Abbreviations are the same as Fig. 3.2 and 3.4. The approximate boundaries between formations are indicated by dashed lines. Group names, the key group names, flow numbers, flow boundaries and red bole beds are shown. GPB: lava layer including flow of giant plagioclase basalts.

Group V (ST V) comprises flows 21 and 22. This group overlies the marker flow 20 which has high K_2O, P_2O_5, Ba, Zr abundance. It is capped by the maker flow 23 which contains high MgO, Sr and low P_2O_5, Y. Their composition is of transitional nature from Ambenali to Kolhapur unit of Mahabaleshwar Formation.

Group VI (ST VI) comprises 5 flows from 24 to 28. Chemical signature of this group is of transitional character from Ambenali to Mahabaleshwar Formation.

Group VII (ST VII) comprises 7 flows from 29 to 35. This group is characterized by a distinctive chemical signature marked by the presence of high SiO_2 and MgO and low TiO_2, P_2O_5, Zr and Nb. This is similar to Bushe on the one hand and to Panhala and Desur on the other. The flow sequence below this is of Ambenali composition, therefore this group cannot be considered to represent Bushe. They are, therefore considered to represent Panhala being low in TiO_2 content but are differ from it in their Ba and Sr abundance. These therefore could be considered as transitional from Kolhapur unit of Mahabaleshwar to Panhala Formation.

Group VIII (ST VIII) includes flows from 36 to 38. They are enriched in SiO_2, P_2O_5, Sr, Zr compared to underlying and overlying groups (Fig. 3.4 k). These compositions are similar to both Ambenali and Kolhapur unit of Mahabaleshwar.

Group XI (ST XI) comprises 40 and 41 flows. This group is lying above the maker flow of basaltic andesite (flow 39). The characteristic chemical compositions are small TiO_2 abundance. Chemical composition of this group indicates transitional nature from Panhala to Desur.

Ajanta section (AJ)

This section comprises 5 sparsely to moderately porphyritic plagioclase phyric flows with subordinate augite and olivine. They are mainly of compound type (Fig. 3.5). The flows exhibit a uniform chemical signature and show marginal enrichment in incompatible elements such as K_2O, TiO_2, P_2O_5, Ba, Sr, Zr and Y. Zr/Nb ratios are between 15 to 19 (Fig. 3.4 l). This chemical signature is comparable to Poladpur.

Buldana section (BU)

This section comprises sequence of 8 flows. The lower part mainly comprises compound flows, while the upper part (from flow 3 upward) constrains simple flows only (Fig. 3.5). Rocks are aphyric to sparsely porphyritic with phenocrysts of plagioclase and rare augite. The uppermost flow (BU-08) is relatively enriched in incompatible elements. The remaining flows are closely similar in composition, being characteristically akin to Ambenali composition (Fig. 3.4 m).

Lonar Crater section (LC)

This section comprises 7 flows. However, during this study samples were collected from only 2 flows. Rocks are sparsely porphyritic with plagioclase phenocrysts. Chemical compositions are similar to Poladpur composition.

Chikhali-Khamgaon (CK)

Only 1 sample was collected from this section in this study. This rock is aphyric basalt. Chemical signature shows typical Ambenali affinity.

Akot-Harisal section (P)

This section comprises 22 flows which can be separated into 5 stratigraphic groups (Fig. 3.4 n). Total thickness of lava pile is 720 m. The section is composed of only simple flows (Fig. 3.5).

Group I (P I) is formed of flows 1 to 5. Rocks are aphyric to sparsely porphyritic with plagioclase phenocrysts. These flows exhibit a mixed signature of Poladpur and Ambenali. Flows 1, 4 and 5 are closer to Poladpur, and 2 and 3 to Ambenali.

Group II (P II) comprises flows from No. 6 to 11. This group is capped by overlying maker flow (No. 12) which is sparsely porphyritic with phenocrysts of plagioclase, subordinate augite, and is characterized by low MgO and high P_2O_5, Ba, Zr abundance and low Zr/Nb ratio (Fig. 3.4 n). Rocks of P II group are aphyric to sparsely

porphyritic with plagioclase phenocrysts. The distinctive chemical signature is high SiO_2. Chemical signature of this group is closer to Poladpur.

Group III (P III) comprises flows from 13 to 18. Thickness of this group is 230 m. They are almost aphyric flows. Chemical signature is that of typical Ambenali type.

Group IV (P IV) comprises flows 19 and 20. Rocks are sparsely porphyritic with plagioclase and augite phenocrysts. Chemical composition of this group is similar to underlying P III except for low Zr content. This group appears to represent transitional composition from Ambenali to Mahabaleshwar.

Group V (P V) comprises only one flow (No. 22), overlying the marker flow 21. The composition of marker flow shows mixed signature of Panhala and Desur. Composition of P V group is typical of Ambenali nature.

Chikaldara section (CH)

This section is composed of 25 lava flows within a vertical column of 625 m. Lava flows are thick simple flows, ranging in thickness from 7 to 49 m. In this section, 5 groups are recognized (Fig. 3.4 o). Detail descriptions of this section are shown in Deshmukh *et al.* (1996b).

Group I (CH I) comprises 4 aphyric flows from 1 to 4. This group is capped by the marker flow of CH-5. This marker flow is aphyric to sparsely porphyritic, coarse grained doleritic with phenocrysts of plagioclase, augite and opaque. CH-5 is characterized by the presence of high MgO and low K_2O, P_2O_5, Ba and Zr. Lower two flows of CH I group are characterized by high TiO_2, P_2O_5, Ba, Zr and Y compared to upper two flows. Compositions of upper two flows are similar to Poladpur, while those of lower two flows are enriched in HFS elements.

Group II (CH II) comprises flows from 6 to 11. All rocks are sparsely porphyritic with phenocrysts of plagioclase and rare augite. Composition of flows of this group is ranges widely with some exhibiting high K_2O, P_2O_5, Ba, Sr, Zr and Y abundances. This type of enrichment in incompatible elements is not seen in the upper six formations of Western Ghats area.

Group III (CH III) comprises 16 flows from 12 to 27. Thickness of this group is 268 m. Lower 12 flows and uppermost flow 27 are aphyric to sparsely porphyritic with phenocrysts of plagioclase and augite, while No. 24 and 25 flows are highly porphyritic basalts. Chemical composition is relatively uniform with small K_2O and Ba abundance. This chemical signature is similar to that of Ambenali Formation.

Group IV (CH IV) comprises 4 flows from 28 to 31 which contain conspicuously low TiO_2 in the sequence with high SiO_2. This group is characterized by small TiO_2, P_2O_5, Sr, Zr abundance. This character is closely similar to Panhala. Rocks of this group are highly porphyritic (>20 vol. %) with phenocrysts of plagioclase with subordinate augite.

Group V (CH V) consists of top 5 flows (CH-32 to CH-36). Chemical signature of this group is similar to Ambenali. Rocks are almost aphyric basalts.

Amravati-Nagpur section (AN)

Two samples were collected from this section. Rocks are aphyric to sparsely porphyritic with plagioclase phenocrysts. Compositions of these samples are similar to Ambenali.

Talegaon section (TL)

Samples of two flows were collected from this section. Rocks are sparsely porphyritic basalts. Phenocrysts in TL-01 sample are of olivine, plagioclase and augite and those of TL-52 are plagioclase only. Whole rock compositions of these rocks show similarity with Ambenali.

Kalalgaon-Vaghapur section (KV)

This section comprises 5 flows. Only lowest flow is composed compound type and others are simple flows (Fig. 3.4 p). Samples were collected from lower 4 flows in this study. All rocks are aphyric basalts, and compositions of which are close to Ambenali.

Mahur Ghat section (MG)

This section comprises 7 flows. No. 2 and 4 flows are of compound nature, while others are simple flows (Fig. 3.5). Lava pile is divided into 2 groups on the basis of compositional characters (Fig. 3.4 q).

Group I (MG I) comprises lower 5 flows. No. 5 flow is aphyric, however, No. 3 flow is highly porphyritic with phenocrysts of plagioclase, and subordinate augite. No. 2 and 4 flows are aphyric, coarse grained doleritic basalts. Compositional signature of this group is similar to Poladpur.

Group II (MG II) comprises flow 6 and 7. They are aphyric to sparsely porphyritic with plagioclase phenocrysts. Composition of this group is similar to Ambenali.

Bori section (NY)

Samples were collected from 3 flows in this section. Rocks are aphyric to sparsely porphyritic with phenocrysts of plagioclase, subordinate olivine and augite. These samples are more or less similar in composition excepting relatively enriched nature of NY-02-51 in Ba, Y and Zr. Compositional character is that of typical Ambenali.

Nagpur section (NP)

Three samples from this section were analyzed. Rocks are sparsely porphyritic with plagioclase and augite phenocrysts. Compositional signature of these rocks is of typical Ambenali type excepting for marginally higher Ba content of NP-01-51 and NP-02-51 samples.

Nagpur-Chhindwara section (NC)

Samples were collected from 7 simple flows in this section. Lava pile can be divided into 3 stratigraphic groups (Fig. 3.4 s). Detailed discussion on the stratigraphy of this section has been presented by Yedekar *et al.* (1996). The lava sequence of Nagpur-Chhindwara (NC), Nagpur-Jabalpur (NJ) and Jabalpur-Mandla (JB) sections has been divided into four groups (YA to YD) on the basis of distinctive change in the

incompatible elemental ratios in the stratigraphic succession of flows (Yedekar *et al.* ,1996).

Group I (NC I) comprises flow 1 only. This flow is sparsely porphyritic with plagioclase phenocrysts. Chemical signature shows typical Ambenali affinity.

Group II (YC) comprises 3 flows from 4 to 6. Most rocks are aphyric to sparsely porphyritic, coarse grained doleritic with phenocrysts of plagioclase. Chemical compositions of these rocks show transitional character from Ambenali to Mahabaleshwar.

Group III (YD) comprises uppermost 2 flows. These flows are sparsely to highly porphyritic with phenocrysts of plagioclase, subordinate augite and olivine, which has a typical Mahabaleshwar compositional signature.

Nagpur-Jabalpur section (NJ)

This section comprises 17 simple flows. Samples from lower 15 flows were collected in this study. Five stratigraphic groups are identified on the basis of geochemical variation (Fig. 3.4 t). Detailed discussion on the stratigraphy of this section has been presented by Yedekar *et al.* (1996).

Group I (NJ I) comprises flow 2 only. This flow is sparsely porphyritic with plagioclase phenocrysts. The distinctive compositional signature is very high Ba and Sr abundance.

Group II (YA) comprises 3 flows from 3 to 5 Most rocks are aphyric and some contain minor proportion of plagioclase phenocrysts. Chemical composition of this group shows typical Ambenali affinity.

Group III (YB) comprises flows 6 and 7. No. 7 flow is giant plagioclase basalt (GPB), while No. 6 is aphyric basalt. GPB (No. 7) flow is characterized by high TiO_2, P_2O_5, Zr and Y abundance compare to overlying and underlying flows.

Group IV (YC) comprises 5 flows from 8 to 12. Rocks are sparsely to highly porphyritic with phenocrysts of plagioclase, subordinate olivine or augite and/or augite. Chemical signature is similar to Ambenali.

Group V (YD) comprises 3 flows from 13 to 15. Petrographic and geochemical characters are similar to Group IV (YD).

Jabalpur-Mandla section (JB)

This section comprises 15 simple flows. Wide variation in the chemical composition of the flows is noticed and they are divided into four stratigraphic groups (Fig. 3.4 u). Detailed discussion on the stratigraphy of this section has been presented by Yedekar *et al.* (1996).

Group I (YA) comprises lower 5 flows (JB-1 to JB-2). Rocks are highly porphyritic with phenocrysts of plagioclase and augite. Chemical signature of this group is transitional between Poladpur and Mahabaleshwar. JB-02-52 exhibits very significant enrichment in Ba and Sr.

Group II (YB) comprises flows 6, 7 and 8. JB-10-51 (No. 7 flow) represent GPB flow. This is equivalent to flow 7 of NJ section. Therefore, Group II (YB) may correspond with Group III (YB) of NJ section.

Group III (YC) comprises 4 flows from 9 to 12 Compositions of JB-04-51 (No. 9 flow) are different from those of JB-05-51 (No. 12 flow) because of No. 9 flow being of GPB character.

Group IV (YD) comprises 4 flows from 13 to 16. Rocks are sparsely porphyritic with phenocrysts of plagioclase, rare augite. Chemical character is similar to Ambenali.

Probable stratigraphic framework of the central and eastern Deccan Traps

On the basis of the description presented in the foregoing pages a tentative stratigraphy for the lava pile in the central and eastern sectors is proposed. This stratigraphy is essentially based on the geochemical variations observed in the sections examined. For the purpose of establishing the chemical stratigraphy two distinctive key

groups have been identified. They are recognized in many sections of the central and eastern area.

One key group is thick, chemically homogeneous group, having the chemical signature similar to Ambenali Formation in Western Ghats area. This is named as "Eastern Ambenali Formation" in this study. Thickness of this group for each section is as follows; 275 m of ST IV, > 145 m of BU I, 230 m of P III, 268 m of CH III, > 120 m of KV I, 220 m of MG II, >40 m of NY I, > 115 m of NJ III, > 65 m of JB III. Average chemical composition is SiO_2-49.9, TiO_2-2.45, MgO-6.0, K_2O-0.33, P_2O_5-0.23 (wt.%), Rb-7, Sr-216, Ba-80, Y-36, Zr-162 and Nb-11 (ppm).

Second key group is chemically distinctive with low TiO_2 abundance. Average composition is SiO_2-52.0, TiO_2-1.16, MgO-6.5, K_2O-0.42, P_2O_5-0.11 (wt.%), Rb-11, Sr-184, Ba-146, Y-31, Zr-98 and Nb-6 (ppm). This compositional signature is roughly similar to Bushe, Panhala and Desur formations in Western Ghats area. This group is named "Eastern Low-Ti Formation" in this study. This formation overlies the Eastern Ambenali Formation, directly (at CH section) or indirectly (at ST and P sections) (Fig. 3.5).

The two key groups are seen to have a large regional extent from Toranmal in west to Jabalpur in east. Utilizing the regional extent of these chemically distinct groups in individual sections, it is seen that the total lava pile of this region is divisible into several stratigraphic groups. A schematic representation of this stratigraphy is shown in Fig. 3.5. The author is fully aware that this model needs to be referred and conferred by taking account geological and structural features as well as by providing additional geochemical inputs from systematic field and geochemical study in closely spaced sections across the entire area. It is only then the spatial and temporal continuity of the stratigraphic divisions, recognized during the present work would be property established and understood. Nevertheless, the present work has undoubtedly established presence of chemically distinct stratigraphic groups in several sections almost across the entire spread of the central and eastern Deccan. The present studies have thus provided a first order

stratigraphic model which should serve as a basis for further detailed work on this subject.

IV. Petrological study of Deccan Trap basalts

1. Purpose and previous works

It has been argued that the geochemical features of the Deccan basalts can be explained by two well-developed mixing lines, one between Ambenali magmas and crustal materials, the other between Ambenali magmas and the products of the postulated lithospheric mantles. The Ambenali magmas are regarded to be least contaminated and to be controlled by the degree of gabbro fractionation. These discussions are made based on the studies of basalts only in the Western Ghats (Cox and Hawkesworth, 1984; 1985; Cox and Mitchell, 1988; Devey and Lightfoot, 1986; Lightfoot *et al.*, 1990; Mahoney, 1988; Mahoney *et al.*, 1982; Peng *et al.*, 1994; Sen 1986); however, it is not clear if the similar arguments are applicable to the basalt piles in the central and eastern parts of Deccan.

All previous workers suggested that MgO-rich basalt (MgO > 10 wt.%) was the parental magma of the Ambenali magmas (Aoki *et al.*, 1992; Cox, 1980; Cox and Hawkesworth, 1985; Krishnamurthy and Cox, 1977; Lightfoot *et al.*, 1990; Mahoney, 1988). It was reported that there were sparsely porphyritic MgO-rich basalts which can be in equilibrium with mantle lherzolite in Deccan Traps (Krishnamurthy and Cox, 1977; Melluso *et al.*, 1995; Sen, 1988). However, incompatible element concentrations of all these basalts are enormously higher (*e.g.*, K_2O > 0.8 wt.%, Ba > 150 ppm) than those of the Ambenali magmas. Therefore, the MgO-rich magma is not parental magma of the Ambenali magmas.

Beane and Hooper (1988) have described picrites collected from Western Ghats area. Incompatible element concentrations of the rocks were as low as those of the Ambenali basalts. All those rocks are porphyritic. Moreover, Fo content of olivine phenocryst is lower than 80, suggesting that the magma of these rocks could not have been in equilibrium with mantle lherzolite (Takahashi, 1986b). Beane and Hooper (1988) have suggested that those picritic rocks were cumulate origin. Fo content of olivine

phenocryst in picrites (MgO > 20 wt.%) collected at Alibag-Khopoli area (Fig. 3.2) is also lower than 80 (Appendix C). It can be concluded that no parental picrite of the Ambenali basalts have been sampled in the Deccan Traps.

In spite of this fact, previous workers suggested the existence of virtual parental picrite of the Ambenali magmas. In order to explain the lack of parental picrite at the surface, Cox (1980) proposed fractional crystallization process which generates the concealed cumulates at the base of the crust. However, there is no study to evaluate whether the partial melt of mantle lherzolite could be parental magma of the Ambenali magmas or not.

When we examined these previous works, three questions arise. (1) Can we distinguish uncontaminated magmas like the Ambenali magmas in the central and eastern Deccan as established in the Western Ghats? (2) Do melting experiments support the gabbro fractionation model suggested by Lightfoot *et al.* (1990) to explain the chemical variation of the uncontaminated magmas? (3) Can the uncontaminated magmas be generated by fractional crystallization of magmas formed by partial melting of mantle lherzolites?

Although Deshmukh *et al.* (1996a) argued that the geochemical features of basalts in the central and eastern area are comparable to those in the Western Ghats, it has not been clarified what extent the uncontaminated magmas like the Ambenali magmas in the Western Ghats are distributed. In this chapter, therefore, uncontaminated basalts are distinguished among the basalts in the central and eastern Deccan and the compositional variation within the uncontaminated basalts is discussed based on the one atmosphere melting experiments. Moreover, major and trace element composition of the most primitive magma which is called the pristine magma in the uncontaminated magmas of Deccan Traps will be compared with those of magmas formed by partial melting of mantle lherzolite and subsequent fractional crystallization.

2. Discrimination of the uncontaminated basalts

In the beginning, we have to eliminate the influence of crustal materials or lithospheric mantle components in order to estimate uncontaminated basalts. The uncontaminated basalts are defined, here, as basalts which have no influence of crustal materials or lithospheric mantle components.

Accumulated chemical analyses of Deccan basalts show wide scattering of composition not only in isotopic ratios but also in major and trace element compositions (*e.g.*, Deshmukh *et al.*, 1996). It is impossible to identify any fundamental systematics within the scattered chemical variation. The scattered nature could be due to the influence of crustal or lithospheric mantle components (Cox and Hawkesworth, 1985; Lightfoot and Hawkesworth, 1988; Lightfoot *et al.*, 1990; Mahoney *et al.*, 1982).

In the Western Ghats, it has been argued that most basalts except for basalts of the Ambenali Formation suffered assimilation of crustal materials (*e.g.*, Mahoney *et al.*, 1982) or lithospheric mantle components (*e.g.*, Hooper, 1994). Nd- and Sr-isotopic data is one of the most excellent data to evaluate the influence of crustal materials or lithospheric mantle components. Fig. 4.1 shows Nd- and Sr-isotopic data for Western Ghats area (Cox and Hawkesworth, 1985; Lightfoot and Hawkesworth, 1988; Lightfoot *et al.*, 1990; Mahoney *et al.*, 1982; Peng *et al.*, 1994). It can be recognized two mixing trends: Ambenali-Poladpur-Bushe trend and Ambenali-Panhala-Mahabaleshwar trend. It was proposed that the Ambenali-Bushe trend was generated by contamination of broadly granitic crust (Cox and Hawkesworth, 1985; Lightfoot and Hawkesworth, 1988; Mahoney, 1988). Available Pb- and O-isotopic data are consistent with this interpretation (Lightfoot and Hawkesworth, 1988; Lightfoot *et al.*, 1990; Matsuhisa *et al.*, 1986). The Ambenali-Mahabaleshwar trend has been proposed to reflect the mixing of isotopically Ambenali magmas with one of the ancient granulitic crust component (*e.g.*, Mahoney, 1982), or with continental lithosphelic mantle (*e.g.*, Lightfoot *et al.*, 1990). The question of which component suitable for end member is still controversy. In any case, low ε_{Nd} values and high $^{87}Sr/^{86}Sr$ ratios are accepted as clear lines of evidence of the influence of

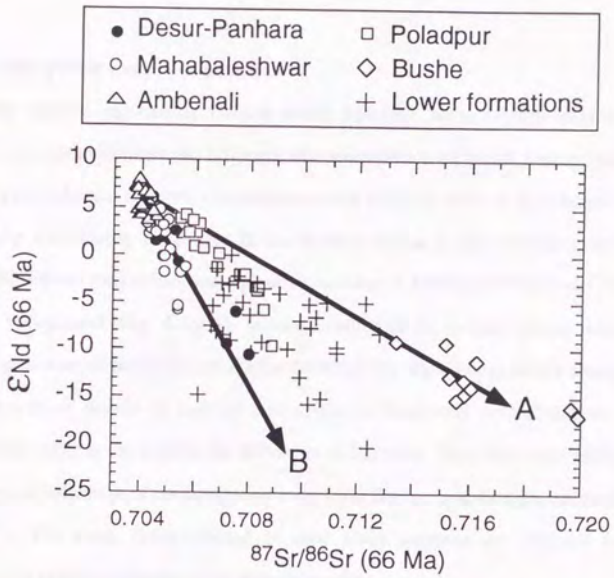

Fig. 4.1 Initial Nd- and Sr-isotope variations in Deccan Trap basalts at 66 Ma. Two mixing lines (A and B) can be observed, both anchored in the field of the Ambenali basalts around $^{87}Sr/^{86}Sr = 0.704$, $\varepsilon_{Nd} = 7$. A: Ambenali-Poladpur-Bushe trend, B: Ambenali-Panhala-Mahabaleshwar trend. It was proposed that end member of trend A is granitic crust and that of trend B is granulitic crust or continental lithosphelic mantle. Abbreviation for each formation is the same as Fig. 3.2. Data are from Cox and Hawkesworth (1985), Lightfoot and Hawkesworth (1988), Lightfoot *et al.* (1990), Mahoney *et al.* (1982) and Peng *et al.* (1994).

crustal or lithospheric source components.

In the central and eastern Deccan areas, however, these isotope data are not available. In order to estimate the influence of contamination on basalt, I have examined several major and trace element concentrations and ratios in relation to isotopic ratios. Through the compilation of the data in the Western Ghats, a clear reverse correlation between Ba/Nb and ε_{Nd} values and a positive correlation between Ba/Nb and $^{87}Sr/^{86}Sr$ ratios are recognized (Fig. 4.2a, b). Incompatibility of Ba to each phase related to magmatic processes of basalt is very similar to that of Nb. Ba/Nb ratio hardly changes by the differences of degree of melting and degree of fractional crystallization. Only contamination process can explain the difference of this ratio. Therefore, this ratio can be used as a good indication of contamination even when the isotopic data are not available. In Fig. 4.2, The term, contaminated, is used when magmas are affected by the components of crustal materials or lithospheric mantle.

The obviously contaminated basalts must have less ε_{Nd} values and larger $^{87}Sr/^{86}Sr$ ratios than those of primitive mantle at 66 Ma ($\varepsilon_{Nd} = 0$, $^{87}Sr/^{86}Sr = 0.7050$). In this study, the rocks which have Ba/Nb > 10.0 are regarded as contaminated basalts (Fig. 4.2a, b). The contaminated basalts, thus defined, correspond to basalts with ε_{Nd} value less than 0 and $^{87}Sr/^{86}Sr$ ratio larger than 0.7050. While almost of contaminated rocks ($\varepsilon_{Nd} < 0$ and $^{87}Sr/^{86}Sr > 0.7050$) could be discriminated by Ba/Nb ratios, some contaminated basalts ($\varepsilon_{Nd} < 0$ and $^{87}Sr/^{86}Sr > 0.7050$) of Desur, Panhala and Lower Formations can not be detected by this ratio (Fig. 4.2a, b). Previous workers suggested that Desur and Panhala magmas were originated in the subcontinental lithosphere (Lightfoot *et al.*, 1990). These basalts are characterized by their low TiO_2 contents (Table 3.1). On the other hand, isotopically uncontaminated basalts have high TiO_2 contents (>1.95 wt.%). Therefore, the rocks which have $TiO_2 \leq 1.95$ wt % can be also regarded as contaminated basalts (Fig. 4.2 c).

According to the above discrimination methods (Ba/Nb ratio and TiO_2 content), all Deccan Trap basalts which include the central and eastern Deccan basalts were divided into two groups, the contaminated and the uncontaminated basalts. Fig. 4.3 shows

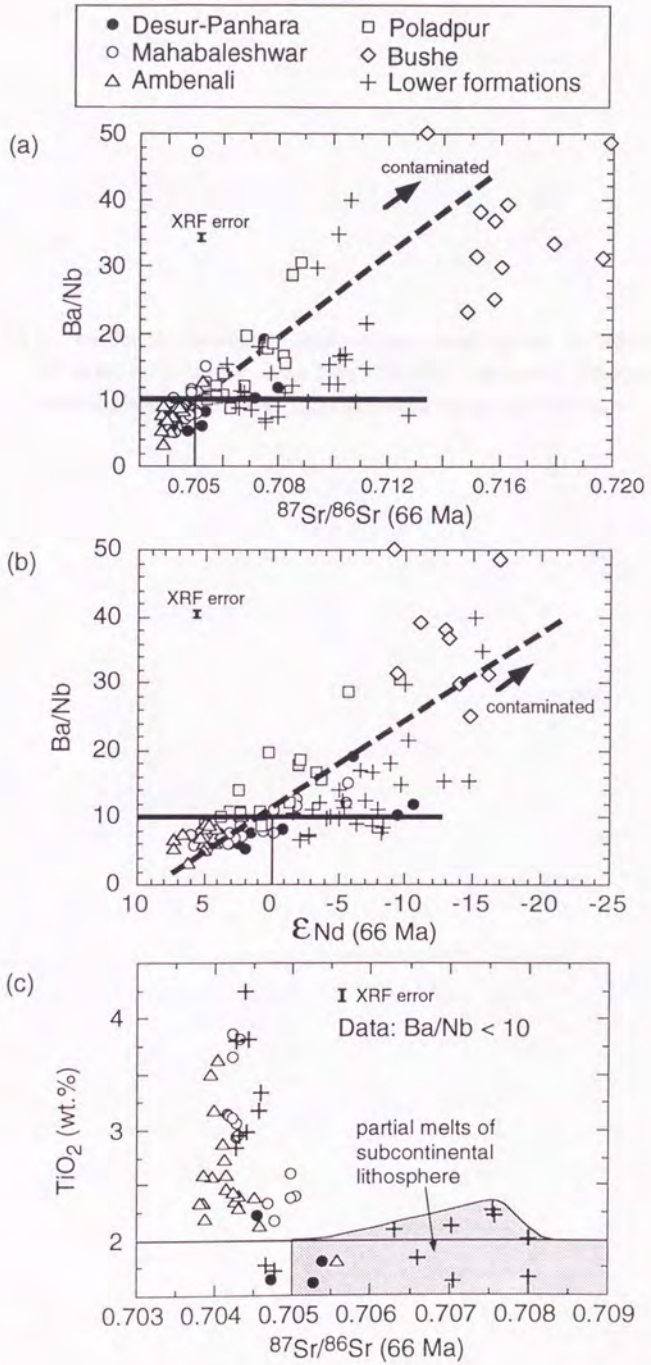

Fig. 4.2 (See next page for explanations)

Fig. 4.2 (--- continued) Variation in (a) Sr-isotope versus Ba/Nb, (b) Nd-isotope versus Ba/Nb and (c) Sr-isotope versus TiO_2 in Deccan Trap basalts. Abbreviation for each formation is the same as Fig. 3.2. Data sources are the same as Fig. 4.1.

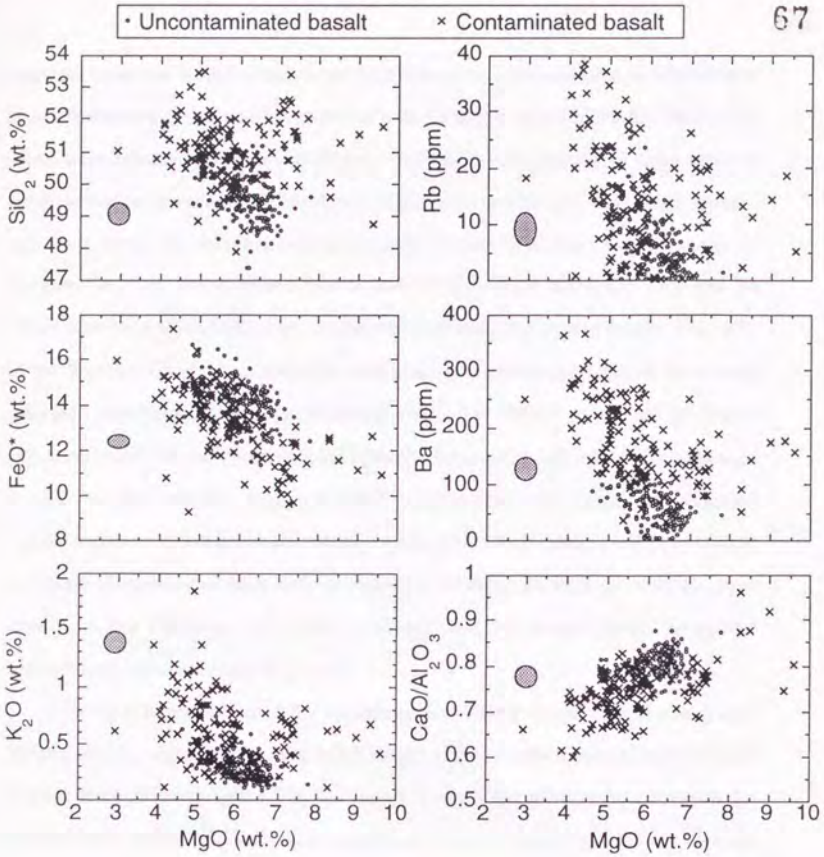

Fig. 4.3 Plots of selected major and trace elements versus MgO for Deccan Trap basalts. XRF error: The 2 sigma ellipse is the calculated standard deviation of the mean for XRF analyses of 10 rocks collected from a single lava flow (MA-W).

chemical variations in selected major and trace element compositions against MgO. Major and trace element analyses were carried out with the Rigaku System 3080ES XRF of the Earthquake Research Institute, University of Tokyo. The major and trace element compositions are presented in Table A2a. Contaminated basalts have wide range in major and trace elements, whereas uncontaminated basalts have very limited range of composition. The contaminated basalts have slightly high SiO_2, K_2O, Rb and Ba contents and low CaO/Al_2O_3 ratios compared to the uncontaminated basalts (Fig. 4.3). In the Western Ghats, these chemical characters of contaminated basalts have been reported by previous workers (*e.g.,* Mahoney, 1988). It is difficult to evaluate the degree of contamination for each contaminated basalts because composition of the contaminant is unknown. Nevertheless, Mahoney (1988) compiled previous works and suggested that the highly modified Bushe lavas could have acquired their isotopic and most of their elemental characteristics from bulk incorporation of about 20 wt.% of Archean upper crust. Cox and Hawkesworth (1984) concluded that the average crustal input into contaminated basalt is around 6-12 wt.%.

Chemical compositions of the uncontaminated basalts in the eastern and central Deccan area are very similar to those in the basalts of the Ambenali Formation (Ambenali basalts) at the Western Ghats. Fig. 4.4 shows stratigraphic relationships between the contaminated and the uncontaminated basalts of whole Deccan Traps. On the Western Ghat area, the uncontaminated basalts form thick lava pile (> 500 m) which is defined as Ambenali Formation. The uncontaminated basalts in the central and eastern area are also recognized as thick (> 200 m) continuous lava pile (Fig. 4.4). They roughly correspond to stratigraphically defined "Eastern Ambenali Formation" (chapter III). The ratio of total thickness was calculated by comparing the total thickness of uncontaminated lavas with that of contaminated lavas. Total thickness of the uncontaminated basalts is estimated to be 51 % in the whole sections. This fact indicates that the uncontaminated basalts constitute a major proportion of the Deccan Trap lava pile.

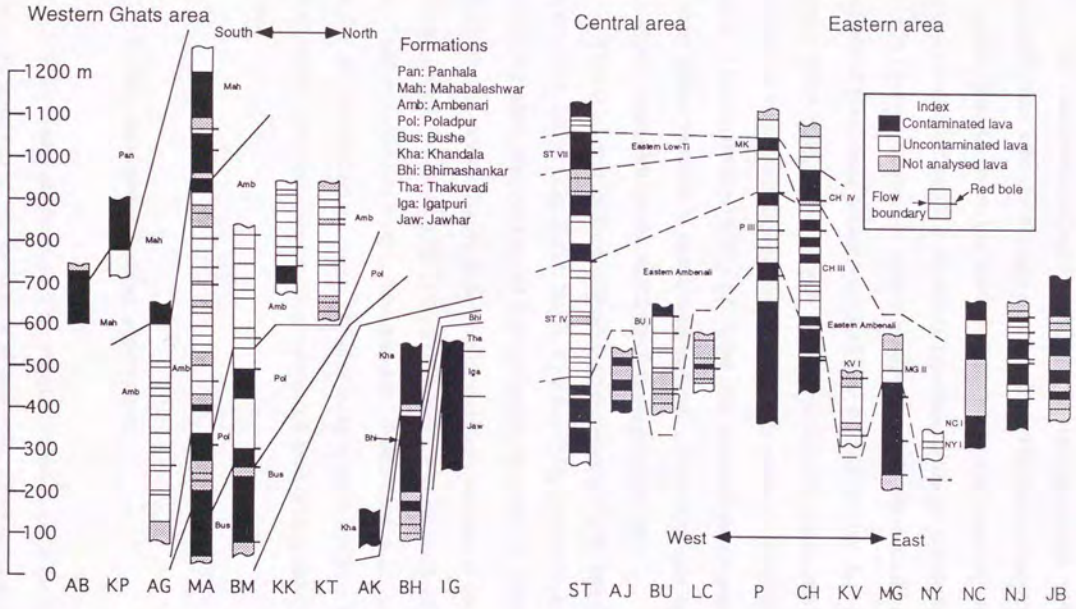

Fig. 4.4 Section showing the spacing relationships between contaminated and uncontaminated rocks through the all Deccan Traps. The columnar sections are the same as Fig. 3.3 and 3.5. The approximate boundaries between formations are indicated by solid lines for Western Ghats area and dashed lines for central and eastern area. Group names, the key group names, flow numbers, flow boundaries and red bole beds are shown. GPB: Lava layer including flow of giant plagioclase basalts. Abbreviation of each section is same as Fig. 3.2.

3. Chemical variation of the uncontaminated basalts

The uncontaminated basalts are aphyric to highly porphyritic rocks. Phenocrysts are plagioclase, subordinate augite and rare olivine. Phenocryst content varies from 0 to 30 vol.%. Fig. 4.5 shows that most of highly porphyritic basalts are akin to aphyric-sparsely porphyritic basalts in chemical composition. A few porphyritic basalts have high Al_2O_3 content compared to aphyric basalts (Fig. 4.5). These basalts contain a large volume of plagioclase phenocrysts (> 15 vol. %). This fact can be explained by the accumulation of plagioclase crystals. The other porphyritic basalts also may have been affected by the accumulation of plagioclase crystals, while we can not discriminate the effect of the accumulation in Fig. 4.5. As we want to discuss the process to generate the compositional variation of liquid, compositional variations of only aphyric-sparsely porphyritic basalts will be discussed in the following discussions.

The major element compositions of aphyric basalts display certain fundamental systematics: SiO_2, TiO_2, FeO*, Na_2O, K_2O and P_2O_5 progressively increase with decreasing MgO, and Al_2O_3 and CaO progressively decrease; incompatible trace elements, *e.g.*, Rb, Sr, Ba, Y, Zr and Nb progressively increase in the same way; Cr and Ni abruptly decrease (Fig. 4.5). These chemical trends may be explained by fractional crystallization process. The candidates of subtracted phases are phenocrystic phases such as plagioclase, augite and olivine. In order to evaluate this possibility quantitatively, one atmosphere melting experiments have been conducted as described below.

4. One atmosphere melting experiments

In order to evaluate the cause of the chemical variation within the uncontaminated basalts, the liquid line of descent (LLD) of the magnesian uncontaminated basalt has been estimated through the one atmosphere melting experiments. Similar attempts have been

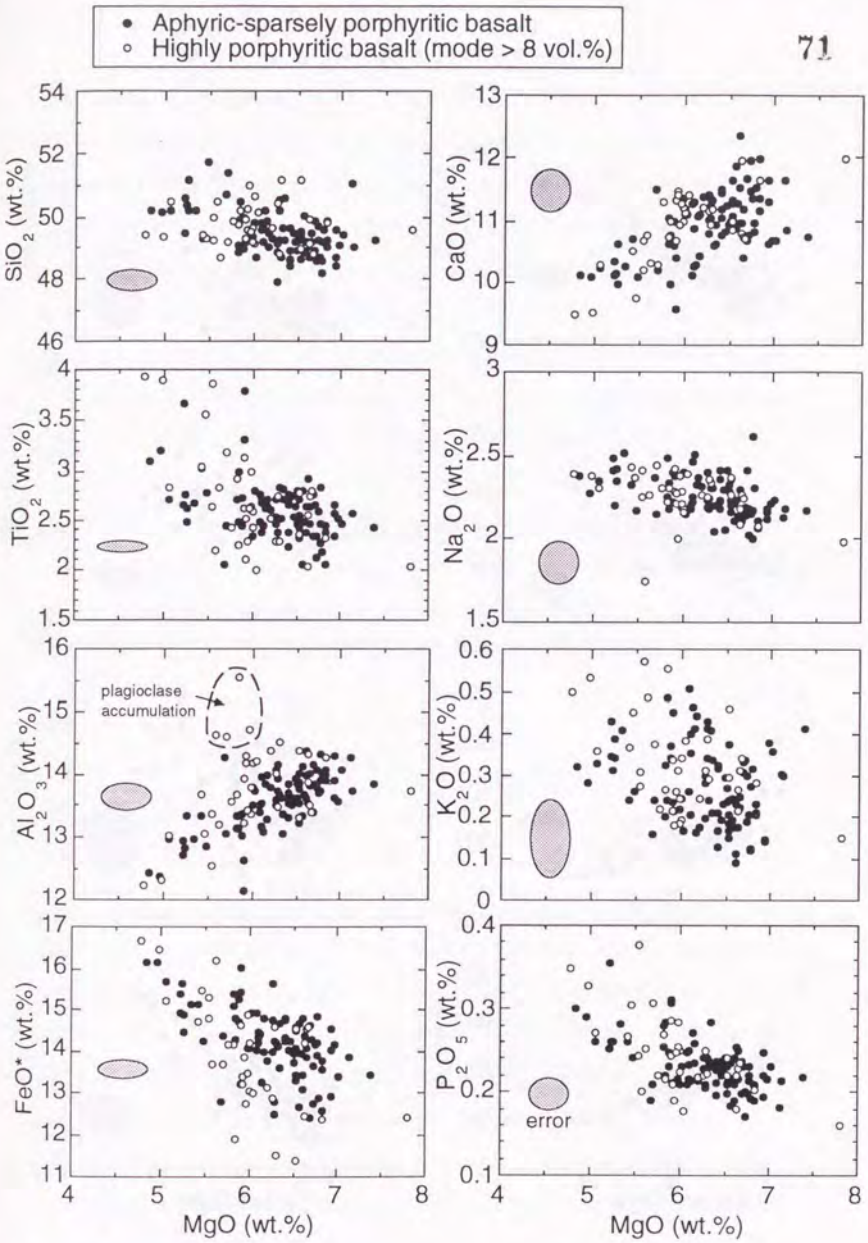

Fig. 4.5 Plots of major and selected trace elements versus MgO for the uncontaminated basalts which are defined based on Ba/Nb ratios and TiO_2 contents for Deccan Trap basalts. XRF error: Ellipses represent the standard deviations of 2 sigma of XRF analyses for 10 specimens from one outcrop (MA-W).

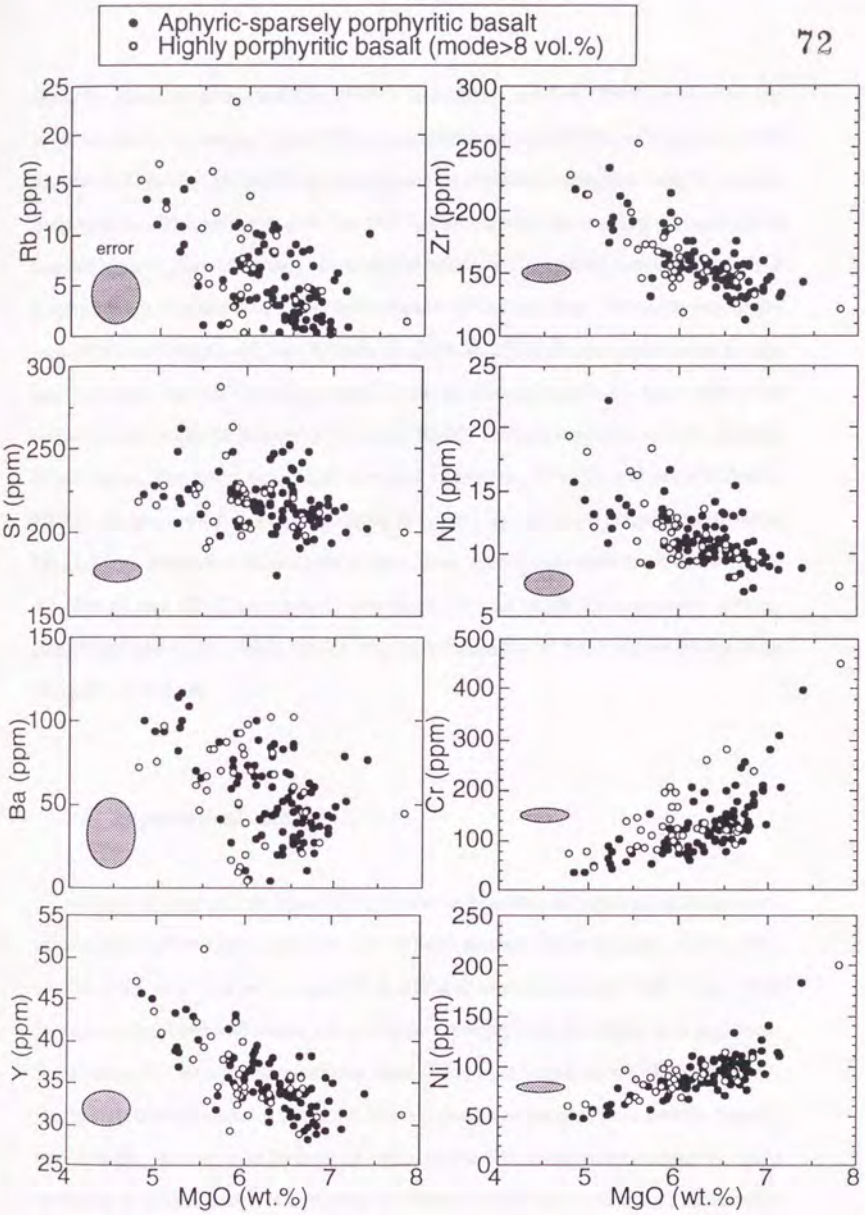

Fig. 4.5 (--- continued)

made by Krishnamurthy and Cox (1977), and Cohen and Sen (1994). However, the experiments by Cohen and Sen (1994) were conducted at 0.6 GPa and they concluded that the LLD at high pressure was not adequate to explain the chemical trend of Deccan Trap basalts. Krishnamurthy and Cox (1977) also reported the melting experiments at one atmosphere. However, they chose alkalic basalts as the starting materials, and their results are not applicable to the tholeiitic basalts of Deccan Trap. Therefore, one of the most MgO-rich (MgO = 6.7 wt.%) tholeiite (MA-W-25) in the uncontaminated basalts was selected for the melting experiments at one atmosphere. Two MgO-rich contaminated tholeiitic basalts (BH-14 and IG-02) were also selected for the melting experiments. The latter have MgO contents as high as 9 wt.%, and are suitable to identify the phase relation available for the fractional crystallization calculations (chapter IV-5). Major element compositions of these three starting materials are listed in Table 4.1. BH-14 and IG-02 are sparsely olivine phyric and MAW-25 is sparsely olivine, plagioclase and augite phyric basalts. Phenocryst contents of these basalts are less than or equal to 3 vol. %.

A. Experimental method

Samples were cut into about 0.5 to 1.0 cm wide tablets and were crushed into mm-sized pieces. Altered parts were removed by hand-picking. Then, the rock samples were packed with pure acetone in agate ball mill and crushed into powder. These rock powders were dried and about 4.0 g of them were pressed into disks in a pelletizer. Small chips (20-40 mg) removed from these disks, were bound up with Pt wire. In this study, very thin (diameter = 0.05 mm) Pt wires and large samples were used in order to minimize the absorption of Fe from silicate samples. The samples were fused into glass at the higher temperature (1300 °C) than the liquidus in the same oxidation conditions as the target experiments. These glasses were used as starting samples.

The glass beads on Pt loops were suspended in a furnace. Temperature was

Table 4.1 Starting compositions used in one atmosphere experiments. Fused whole rocks were analyzed by EPMA.

Sample	MA-W-25	BH-14	IG-02
Formation	Amb	Kha	Jaw
SiO2	48.90	48.74	51.55
TiO2	2.77	1.09	1.70
Al2O3	13.39	14.60	12.50
FeO*	14.62	12.62	11.11
MnO	0.21	0.17	0.15
MgO	6.69	9.33	9.00
CaO	10.67	10.86	11.50
Na2O	2.19	1.80	1.80
K2O	0.33	0.67	0.55
P2O5	0.24	0.12	0.14
FeO*/MgO	2.19	1.35	1.23
Mg#	44.9	56.9	59.1
CaO/Al2O3	0.80	0.74	0.92

measured during each run using a $Pt/Pt_{87}Rh_{13}$ thermocouple with the junction placed at the position of the sample. Run temperatures are considered accurate to at least ± 1.5 °C. A mixture of CO_2 and H_2, flowing upward through the vertical furnace, was used to maintain oxygen fugacity at quarts-fayalite-magnetite (QFM) and nickel-nickel oxide (NNO) buffer conditions for the sample, MAW-25. These conditions were selected because most tholeiitic basalts are considered to be crystallized at the oxygen fugacity condition between these two buffers (*e.g.*, Helz and Thornber, 1987; Walker *et al.*, 1979). The melting experiments for BH-14 and IG-02 were carried out only at the QFM buffer.

Compositions of mineral phases and glasses were determined by the JXA-8800R EPMA of the Earthquake Research Institute, University of Tokyo, using 15 kV accelerating voltage and 12 nA beam current. Counting time is 10 seconds for all experiments. For analyzing glasses, a defocused electron beam (> 10 μm diameter) was employed in order to minimize volatilization of alkalis during analysis. Experimental run conditions and phase assemblages are listened in Table 4.2. Experimental run duration was varied depending on temperature. In all experiments quenched liquid and olivine and plagioclase crystals were chemically homogeneous. As some augite phenocrysts crystallized at low temperature experiments (< 1120 °C) was chemically heterogeneous, a large defocused electron beam (50 μm diameter) were employed to obtain the averaged composition; however, such the composition was not used for the fractional crystallization calculation (chapter IV-5).

B. Results

Phase assemblage and proportion in the products of the melting experiments are listed in Table 4.2. Glass and mineral compositions of the melting experiments are listed in Table 4.3. Olivine, plagioclase and augite crystallize simultaneously at about 1155 °C at both QFM and NNO buffers in the uncontaminated basalt (MAW-25). Only these

Table 4.2 One atmosphere experimental conditions and phase assemblages.

Sample name	Run No.	T (°C)	fO2	Duration (hours)	Run produts	Phase proportions
MA-W-25	#22-1	1191	QFM	23	gl	
	#26-1	1163	QFM	44	gl	
	#32-1	1155	QFM	46	gl, ol, pl, cp	91:1:6:2
	#36-1	1134	QFM	48	gl, ol, pl	81:6:13
	#25-1	1124	QFM	44	gl, ol, pl, cp	61:8:23:8
	#37-1	1119	QFM	61	gl, ol, pl, cp	51:5:27:17
	#35-1	1114	QFM	52	gl, ol, pl, cp	49:5:27:19
MA-W-25	#3-1	1204	NNO	19	gl	
	#23-1	1191	NNO	26	gl	
	#15-1	1170	NNO	48	gl	
	#29-1	1163	NNO	22	gl	
	#2-1	1154	NNO	27	gl, ol, pl, cp, sp	94:tr:6:tr:tr
	#33-1	1144	NNO	47	gl, pl, cp, sp	70:13:14:3
	#18-1	1134	NNO	54	gl, pl, cp, pig, sp	47:27:13:8:5
	#28-1	1123	NNO	45	gl, pl, cp, pig, sp	40:30:17:9:6
BH-14	#6-1	1225	NNO	26	gl	
	#38-1	1214	QFM	26	gl, ol	96:4
	#31-1	1190	QFM	22	gl, ol	94:6
	#34-1	1175	QFM	32	gl, ol, pl, cp	78:10:12:tr
	#26-2	1163	QFM	44	gl, ol, pl, cp	68:14:18:tr
	#24-2	1144	QFM	46	gl, ol, pl, cp	41:16:30:13
	#25-2	1124	QFM	44	gl, ol, pl, cp	29:19:36:16
	#35-2	1114	QFM	52	gl, ol, pl, cp, sp	22:19:39:20:tr
IG-02	#39-1	1232	QFM	27	gl	
	#38-2	1214	QFM	26	gl, ol	100:tr
	#31-2	1190	QFM	22	gl, ol, cp	95:5
	#34-2	1175	QFM	32	gl, ol, cp	86:3:11
	#32-2	1155	QFM	46	gl, ol, pl, cp	79:4:tr:17
	#36-2	1134	QFM	48	gl, ol, pl, cp, pig	47:9:19:25:tr
	#37-2	1119	QFM	61	gl, ol, pl, cp, pig	30:4:19:37:tr

Abbreviations used: gl=glass, ol=olivine,
pl=plagioclase, cp=clinopyroxene, pig=pigionite, sp=spinel, tr: <1

Table 4.3 Electron microprobe analyses of run products of one atmosphere experiments reported in Table 4.2.

MA-W-25 (fO2=QFM)											
gl	T(°C)	n	SiO2	TiO2	Al2O3	FeO*	MgO	CaO	Na2O	K2O	Mg#
#26-1	1163	6	49.74	2.74	13.61	14.31	6.66	10.51	2.17	0.26	45.3
			0.29	0.09	0.22	0.20	0.11	0.22	0.10	0.02	
#32-1	1155	6	49.72	2.87	13.13	14.94	6.40	10.59	2.11	0.26	43.3
			0.30	0.06	0.12	0.46	0.09	0.15	0.13	0.01	
#36-1	1134	6	50.76	3.38	12.18	14.92	5.60	10.73	2.09	0.34	40.1
			0.30	0.10	0.20	0.36	0.14	0.14	0.10	0.02	
#25-1	1124	5	50.77	4.24	11.30	16.40	4.83	9.60	2.39	0.47	34.4
			0.45	0.40	0.08	0.71	0.25	0.11	0.04	0.02	
#37-1	1119	6	48.87	4.36	10.84	19.29	4.57	9.43	2.20	0.45	29.7
			0.37	0.35	0.20	0.45	0.17	0.19	0.13	0.04	
#35-1	1114	6	48.90	4.82	10.69	19.21	4.35	9.40	2.14	0.49	28.8
			0.22	0.07	0.24	0.46	0.13	0.07	0.10	0.04	

ol	T(°C)	n	SiO2	TiO2	Al2O3	FeO*	MgO	CaO	Na2O	K2O	Mg#
#32-1	1155	4	37.49			24.85	37.35	0.31			72.8
			0.26			0.35	0.29	0.02			
#36-1	1134	4	37.40			26.80	35.44	0.36			70.2
			0.48			0.90	0.57	0.06			
#25-1	1124	3	37.00			29.83	32.72	0.45			66.2
			0.41			1.05	1.28	0.02			
#37-1	1119	4	35.95			34.53	29.20	0.33			60.1
			0.35			0.52	0.10	0.02			
#35-1	1114	2	35.75			35.26	28.62	0.37			59.1
			0.11			0.90	0.45	0.01			

pl	T(°C)	n	SiO2	TiO2	Al2O3	FeO*	MgO	CaO	Na2O	K2O	An
#32-1	1155	4	51.99	0.09	29.52	0.82	0.22	13.95	3.34	0.07	69.8
			0.35	0.03	0.12	0.07	0.01	0.21	0.04	0.01	
#36-1	1134	4	52.74	0.10	28.98	0.91	0.26	13.40	3.52	0.09	67.8
			0.62	0.01	0.27	0.09	0.02	0.35	0.15	0.01	
#25-1	1124	4	52.56	0.12	28.59	1.34	0.32	13.34	3.64	0.09	66.9
			0.44	0.02	0.33	0.22	0.04	0.22	0.11	0.01	
#37-1	1119	4	53.14	0.14	28.33	1.34	0.18	12.96	3.78	0.13	65.5
			0.31	0.03	0.54	0.13	0.04	0.20	0.07	0.01	
#35-1	1114	4	53.37	0.15	28.19	1.44	0.21	12.72	3.78	0.14	65.0
			0.20	0.04	0.23	0.04	0.03	0.10	0.17	0.02	

cp	T(°C)	n	SiO2	TiO2	Al2O3	FeO*	MgO	CaO	Na2O	K2O	Mg#
#32-1	1144	3	50.27	1.09	3.50	11.48	17.93	15.59	0.14		73.6
			1.23	0.27	1.14	0.73	0.94	1.29	0.02		
#25-1	1124	3	50.08	1.52	2.93	13.54	15.66	16.03	0.24		67.3
			0.60	0.23	0.33	1.15	0.24	1.53	0.01		
#37-1	1119	4	50.02	1.24	3.73	13.30	15.98	15.52	0.21		68.2
			1.64	0.35	1.79	1.39	0.73	1.22	0.04		
#35-1	1114	3	49.34	1.59	4.77	13.69	15.43	14.98	0.20		66.8
			1.99	0.57	2.60	1.19	0.44	0.74	0.03		

sp	T(°C)	n	SiO2	TiO2	Al2O3	FeO*	MgO	CaO	Na2O	K2O	Cr2O3
#35-1	1114	2	0.17	20.77	3.30	70.31	3.94	0.21			1.30
			0.01	0.17	0.04	0.78	0.11	0.01			0.05

Table 4.3 (--- continued)

MA-W-25 (fO2=NNO)											
gl	T(°C)	n	SiO2	TiO2	Al2O3	FeO*	MgO	CaO	Na2O	K2O	Mg#
#2-1	1154	6	49.60	2.99	12.61	14.70	7.08	10.33	2.35	0.34	46.2
			0.22	0.02	0.21	0.41	0.09	0.24	0.04	0.02	
#33-1	1144	6	51.70	2.76	12.93	14.70	5.54	9.33	2.47	0.58	40.2
			0.27	0.14	0.18	0.31	0.15	0.09	0.07	0.23	
#18-1	1134	4	52.47	3.64	11.81	14.27	5.26	9.85	2.23	0.48	39.6
			0.32	0.09	0.16	0.54	0.12	0.11	0.05	0.02	
#28-1	1123	6	54.23	3.82	11.88	13.70	4.52	8.81	2.47	0.58	37.0
			0.53	0.16	0.24	0.50	0.12	0.11	0.21	0.02	
ol	T(°C)	n	SiO2	TiO2	Al2O3	FeO*	MgO	CaO	Na2O	K2O	Mg#
#2-1	1154	3	37.63			20.95	41.14	0.28			77.8
			0.47			0.29	0.51	0.06			
pl	T(°C)	n	SiO2	TiO2	Al2O3	FeO*	MgO	CaO	Na2O	K2O	An
#2-1	1154	3	52.15	0.08	28.14	2.13	0.28	13.70	3.43	0.09	68.8
			0.92	0.01	2.35	0.62	0.01	0.13	0.01	0.02	
#33-1	1144	4	51.98	0.11	29.06	1.30	0.23	13.78	3.31	0.24	69.7
			0.59	0.02	0.95	0.46	0.03	0.44	0.07	0.09	
#18-1	1134	3	52.91	0.19	27.08	2.51	0.39	13.21	3.59	0.12	67.0
			0.45	0.04	0.66	0.03	0.06	0.32	0.18	0.01	
#28-1	1123	3	53.67	0.19	27.72	1.81	0.26	12.47	3.79	0.11	64.5
			0.39	0.08	0.52	0.21	0.07	0.38	0.13	0.03	
cp	T(°C)	n	SiO2	TiO2	Al2O3	FeO*	MgO	CaO	Na2O	K2O	Mg#
#33-1	1144	3	51.26	0.79	3.43	10.28	17.11	16.91	0.22		74.8
			0.72	0.08	0.61	0.72	0.75	0.37	0.02		
#18-1	1134	1	52.18	1.66	5.41	11.43	13.08	15.77	0.47		67.1
#28-1	1123	3	50.30	1.33	3.31	12.37	14.99	17.46	0.24		68.4
			0.86	0.12	0.29	0.64	0.81	1.41	0.03		
pig	T(°C)	n	SiO2	TiO2	Al2O3	FeO*	MgO	CaO	Na2O	K2O	Mg#
#18-1	1134	1	53.92	0.35	0.79	17.24	24.06	3.59	0.05		71.3
#28-1	1123	2	53.12	0.59	1.28	16.50	22.93	5.52	0.06		71.2
			1.16	0.35	0.69	1.04	1.60	2.71	0.02		
sp	T(°C)	n	SiO2	TiO2	Al2O3	FeO*	MgO	CaO	Na2O	K2O	Cr2O3
#33-1	1144	2	0.16	9.67	5.60	76.25	5.74	0.18			2.40
			0.07	0.08	0.04	0.33	0.19	0.01			0.01
#18-1	1134	3	0.18	9.26	3.74	81.36	5.02	0.19			0.25
			0.02	0.13	0.16	0.61	0.14	0.02			0.05
#28-1	1123	3	0.13	12.43	3.42	79.02	4.72	0.12			0.16
			0.02	0.14	0.01	0.50	0.17	0.02			0.02

Table 4.3 (--- continued)

BH-14 (fO2=QFM)											
gl	T(°C)	n	SiO2	TiO2	Al2O3	FeO*	MgO	CaO	Na2O	K2O	Mg#
#38-1	1214	5	50.15	1.19	15.13	11.25	8.20	11.64	1.91	0.53	56.5
			0.572	0.049	0.102	0.237	0.112	0.248	0.034	0.013	
#31-1	1190	4	50.56	1.17	15.13	11.42	7.50	11.87	1.82	0.53	53.9
			0.334	0.031	0.153	0.276	0.178	0.18	0.047	0.031	
#34-1	1175	6	51.16	1.57	13.82	12.56	6.70	11.52	1.99	0.68	48.7
			0.524	0.066	0.149	0.24	0.118	0.256	0.055	0.026	
#26-2	1163	6	52.37	1.67	13.03	12.56	6.01	11.58	2.00	0.78	46.0
			0.303	0.081	0.216	0.397	0.134	0.26	0.121	0.046	
#24-2	1144	6	51.99	2.52	12.68	15.08	4.91	9.68	2.05	1.09	36.7
			0.597	0.079	0.24	0.481	0.092	0.183	0.058	0.062	
#25-2	1124	6	54.13	2.99	12.85	13.75	4.06	8.25	2.33	1.64	34.5
			0.366	0.103	0.144	0.491	0.081	0.193	0.017	0.019	
#35-2	1114	2	53.88	3.32	12.80	14.05	3.77	8.09	2.16	1.93	32.4
			1.614	0.123	0.216	0.252	0.295	0.411	0.022	0.13	

ol	T(°C)	n	SiO2	TiO2	Al2O3	FeO*	MgO	CaO	Na2O	K2O	Mg#
#38-1	1214	4	38.86			16.90	43.86	0.38			82.2
			0.44			0.302	0.373	0.032			
#31-1	1190	1	38.91			17.52	43.26	0.31			81.5
#34-1	1175	4	38.11			19.98	41.56	0.35			78.8
			0.471			0.847	0.615	0.055			
#26-2	1163	4	38.49			21.67	39.48	0.36			76.5
			0.152			0.164	0.457	0.031			
#24-2	1144	3	37.18			28.68	33.75	0.39			67.7
			0.225			0.355	0.26	0.031			
#25-2	1124	3	36.89			30.31	32.42	0.40			65.6
			0.268			0.329	0.438	0.071			
#35-2	1114	3	36.77			32.48	30.34	0.41			62.5
			0.292			0.225	0.667	0.026			

pl	T(°C)	n	SiO2	TiO2	Al2O3	FeO*	MgO	CaO	Na2O	K2O	An
#34-1	1175	4	50.46	0.05	30.25	0.94	0.31	15.13	2.72	0.14	75.5
			0.42	0.025	0.337	0.238	0.024	0.138	0.16	0.022	
#26-2	1163	4	51.22	0.06	29.86	1.13	0.37	14.41	2.80	0.15	74.0
			0.199	0.016	0.286	0.158	0.041	0.271	0.08	0.009	
#24-2	1144	3	51.07	0.06	30.22	1.30	0.22	14.19	2.74	0.20	74.1
			0.291	0.006	0.315	0.102	0.01	0.65	0.096	0.01	
#25-2	1124	3	51.67	0.07	28.85	1.58	0.38	14.11	3.07	0.27	71.7
			0.32	0.032	0.569	0.175	0.05	0.394	0.153	0.066	
#35-2	1114	3	52.85	0.11	28.68	1.31	0.19	12.94	3.50	0.42	67.1
			0.482	0.03	0.329	0.175	0.04	0.177	0.034	0.032	

cp	T(°C)	n	SiO2	TiO2	Al2O3	FeO*	MgO	CaO	Na2O	K2O	Mg#
#34-1	1175	2	51.56	0.43	3.60	7.67	18.47	18.08	0.16	0.03	81.1
			0.337	0.022	0.165	0.617	0.502	0.861	0.014	0.007	
#26-2	1163	2	51.91	0.83	3.44	8.02	15.38	20.21	0.20	0.01	77.4
			0.417	0.092	0.247	0.014	0.855	0.353	0.007	0.014	
#24-2	1144	3	51.57	0.76	2.72	10.50	15.22	19.02	0.19	0.02	72.1
			0.344	0.133	0.446	0.709	0.247	0.566	0.02	0.015	
#25-2	1124	3	50.46	1.14	3.07	12.14	14.24	18.72	0.22	0.01	67.6
			1.127	0.283	0.586	0.405	0.623	1.076	0.036	0.006	
#35-2	1114	1	51.08	1.02	2.59	12.17	14.89	17.97	0.24	0.04	68.6

Table 4.3 (--- continued)

IG-02 (fO2=QFM)

gl	T(°C)	n	SiO2	TiO2	Al2O3	FeO*	MgO	CaO	Na2O	K2O	Mg#
#38-2	1214	6	51.75	1.75	12.79	11.07	8.31	11.88	1.87	0.58	57.23
			0.29	0.05	0.23	0.46	0.08	0.19	0.10	0.02	
#31-2	1190	4	52.30	1.82	13.12	10.75	7.29	12.15	1.95	0.62	54.72
			0.18	0.09	0.34	0.50	0.15	0.19	0.06	0.04	
#34-2	1175	6	52.68	1.78	14.38	10.76	6.73	10.72	2.22	0.73	52.71
			0.40	0.09	0.33	0.30	0.13	0.21	0.07	0.03	
#32-2	1155	6	52.93	1.91	15.07	10.75	6.01	10.03	2.58	0.72	49.91
			0.56	0.09	0.18	0.27	0.17	0.25	0.13	0.06	
#36-2	1134	6	54.55	3.04	13.13	12.43	4.60	8.54	2.43	1.28	39.74
			0.23	0.06	0.06	0.51	0.06	0.22	0.08	0.04	
#37-2	1119	3	54.09	3.34	13.15	13.37	3.88	7.52	2.79	1.86	34.09
			0.48	0.01	0.09	0.76	0.16	0.25	0.06	0.15	

ol	T(°C)	n	SiO2	TiO2	Al2O3	FeO*	MgO	CaO	Na2O	K2O	Mg#
#38-2	1214	4	39.20			15.92	44.52	0.36			83.29
			0.74			0.64	0.70	0.02			
#31-2	1190	2	39.33			17.52	42.78	0.37			81.31
			0.28			0.02	0.95	0.04			
#34-2	1175	4	38.67			18.69	42.31	0.33			80.14
			0.51			0.20	0.80	0.03			
#32-2	1155	2	38.07			20.22	41.43	0.28			78.50
			0.21			0.48	0.04	0.02			
#36-2	1134	4	37.81			26.57	35.26	0.36			70.28
			0.29			1.16	0.41	0.02			
#37-2	1119	4	36.99			28.25	34.52	0.24			68.53
			0.73			1.12	0.49	0.01			

pl	T(°C)	n	SiO2	TiO2	Al2O3	FeO*	MgO	CaO	Na2O	K2O	An
#32-2	1155	4	52.65	0.08	29.30	0.83	0.29	13.04	3.65	0.16	66.4
			0.50	0.02	0.37	0.04	0.03	0.52	0.18	0.01	
#36-2	1134	4	52.71	0.11	28.83	1.26	0.34	13.09	3.42	0.24	67.9
			0.21	0.02	0.23	0.18	0.07	0.35	0.23	0.04	
#37-2	1119	4	53.44	0.15	28.44	1.18	0.22	12.37	3.89	0.31	63.7
			0.13	0.02	0.36	0.06	0.03	0.16	0.06	0.04	

cp	T(°C)	n	SiO2	TiO2	Al2O3	FeO*	MgO	CaO	Na2O	K2O	Mg#
#31-2	1190	2	53.02	0.61	3.32	6.69	19.09	17.13	0.14		83.57
			0.08	0.06	0.02	0.74	0.12	0.13	0.02		
#34-2	1175	2	52.92	0.56	2.86	7.15	19.07	17.25	0.19		82.62
			0.23	0.00	0.06	0.62	0.46	1.38	0.07		
#32-2	1155	3	51.06	0.90	4.65	6.95	16.85	19.40	0.19		81.21
			0.46	0.20	0.67	0.56	1.46	1.77	0.03		
#36-2	1134	3	50.92	1.38	3.79	9.42	15.07	19.21	0.21		74.03
			0.72	0.37	0.76	0.50	0.34	0.01	0.03		
#37-2	1119	4	49.35	1.36	6.19	10.08	16.71	16.08	0.23		74.71
			0.66	0.25	0.67	0.40	0.03	0.69	0.01		

pig	T(°C)	n	SiO2	TiO2	Al2O3	FeO*	MgO	CaO	Na2O		Mg#
#36-2	1134	1	54.85	0.31	0.69	15.88	24.65	3.59	0.03		73.45
#37-2	1119	1	52.66	0.59	1.17	17.98	22.12	5.36	0.12		68.68

three minerals crystallize even at lower temperatures as 1114 °C at the QFM buffer. On the contrary, magnetite or ilmenite are stable in addition to the above phases at the NNO buffer. Pigeonite also appears at temperature lower than 1134 °C at the NNO buffer. Since neither pigeonite nor opaque minerals is found as phenocrysts in the uncontaminated basalts, it can be suggested that the NNO buffer is not adequate for the oxidation conditions of the uncontaminated magma.

Olivine is the liquidus phase for BH-14 and IG-02 at about 1220 °C. This is in accord with the petrography of these samples, which bear phenocrysts of olivine alone. Plagioclase and augite simultaneously crystallize at 1175 °C for BH-14. On the other hand, sample IG-02 has augite as second crystallizing phase at 1190 °C, and plagioclase in at 1175 °C. The higher crystallizing temperature of augite for IG-02 may have be due to its higher CaO/Al_2O_3 ratio than BH-14 (Table 4.1).

5. Low pressure fractional crystallization

The uncontaminated basalts typically contain phenocrysts of plagioclase, subordinate augite and rare olivine. Phenocrysts of opaque minerals are not recognized in any uncontaminated basalts. This phenocryst assemblage is consistent with phases appeared through the experiments at the QFM buffer.

Fig. 4.6 shows data obtained by XRF analysis of the uncontaminated basalts, and by EPMA analysis of glass in the melting experiments (MAW-25). Because systematic differences are observed among EPMA and XRF analysis for the same samples, data obtained by EPMA analysis were normalized to XRF data (see Appendix D). Glass compositions at the QFM buffer shows increase in SiO_2, TiO_2, FeO*, Na_2O and K_2O and decrease in Al_2O_3 and CaO with decreasing MgO. The compositional trend observed in the uncontaminated basalts is close to the liquid line of descent (LLD) at the QFM buffer (Fig. 4.6). On the other hand, the LLD at the NNO buffer is apart from the compositional trend of the uncontaminated basalts: FeO contents in the melts of

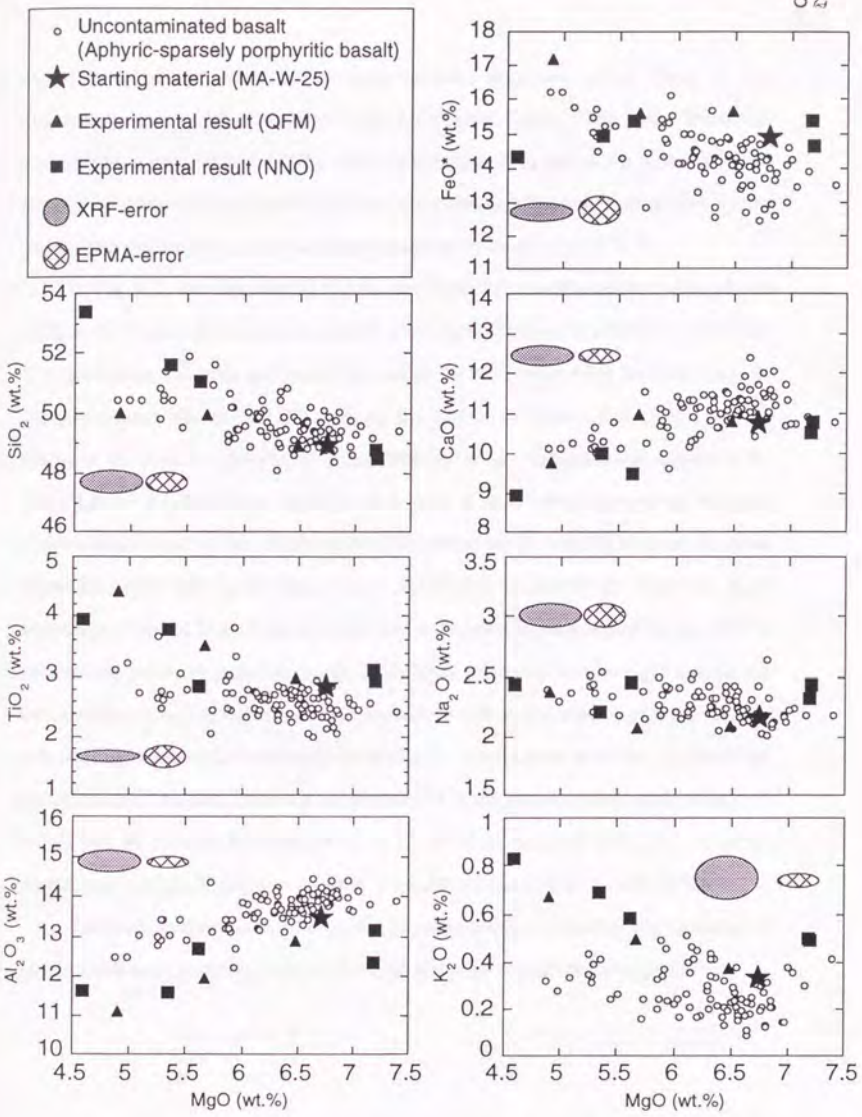

Fig. 4.6 Plots of major elements versus MgO for results of one atmosphere experiments and aphyric rocks of the uncontaminated basalts. XRF error: 2 sigma standard deviations of XRF analyses of 10 specimens collected from one outcrop (MAW), EPMA error: 2 sigma standard deviations of replicate EPMA analyses for LDGO JDFD2 glass.

experiments at the NNO buffer progressively decrease, while those in the uncontaminated basalts increase with decreasing MgO. Therefore, fractional crystallization process at the QFM buffer is favorable than that at the NNO buffer to explain the compositional variation of the uncontaminated basalts. Temperature of the fractional crystallization process is thus estimated to be about 1155-1130 °C.

In Fig. 4.7, the calculated LLD for the fractional crystallization is also shown because the results of melting experiments show the equilibrium crystallization process. The calculation has been performed for one of the most magnesian basalt among the uncontaminated basalts (AN-02) applying the method of Grove *et al.* (1992) and the results of the present experiments at the QFM buffer (see Table 4.4 and Appendix E). The LLD of the fractional crystallization path is in a better agreement with the compositional trend of the uncontaminated basalts in MgO variation diagram for most elements, rather than in the equilibrium experiments on MAW-25. However, K_2O abundance of the LLD is a little different from that of the uncontaminated basalts. This is because the selected primitive basalt (AN-02) is relatively low in K_2O among the uncontaminated basalts. When we select the sample with K_2O content higher than AN-02 as a starting composition, chemical trend of LLD should meet with the cluster of the uncontaminated basalts. Table 4.4 shows that one of the most evolved basalt (MgO = 5 wt.%) can be derived by subtraction of 33 wt.% of minerals (olivine = 4 wt.%, plagioclase = 16 wt.%, augite = 13 wt.%) from AN-02 basalt (MgO = 6.9 wt.%).

The fractional crystallization model has been further applied to the variation of incompatible trace elements using the Rayleigh fractional crystallization equation:

$$\frac{C_i}{C_{i0}} = F^{(D_i - 1)} \qquad (4.1)$$

where, C_i is the concentration of element i in the melt, C_{i0} is the initial concentration of element i in the melt, F is the fraction of melt and D_i is the bulk distribution coefficient of element i between the solid and melt. The mineral/melt distribution coefficients were taken from McKenzie and O'Nions (1991, 1995). The

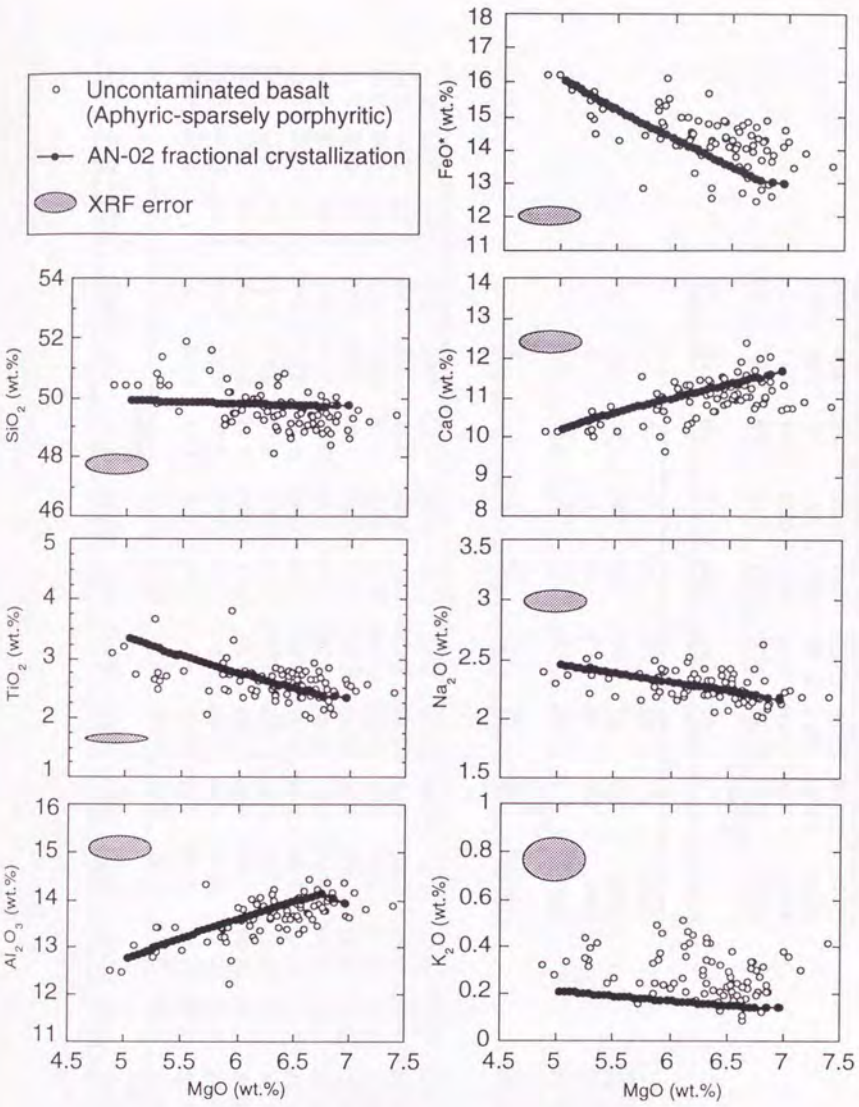

Fig. 4.7 Plots of major elements versus MgO for the aphyric rocks of the uncontaminated basalts. Calculated results fractional crystallization path is also shown from one of the most primitive aphyric rock (AN-02). XRF error: 2 sigma standard deviation of XRF analyses for 10 specimens collected from one outcrop (MA-W), EPMA error: 2 sigma standard deviation of replicate EPMA analyses of LDGO JDFD2 glass.

Table 4.4 Fractional crystallization models for the pristine magma (AN-02) of Deccan Trap basalts. A 1 wt.% sum of equilibrium mineral phases was subtracted from the magma for each step.

sample	SiO2 (wt.%)	TiO2	Al2O3	FeO*	MgO	CaO	Na2O	K2O	P2O5	sub.ol (fraction)	XFo	sub.pl	XAn	sub.cp	XEn
AN-02	49.67	2.34	13.93	12.96	6.94	11.67	2.16	0.14	0.19						
step2	49.62	2.38	14.14	13.06	6.74	11.53	2.20	0.14	0.19	0.01	0.78			0.99	0.80
step3	49.62	2.40	14.11	13.13	6.69	11.50	2.21	0.14	0.20	0.12	0.77	0.50	0.74	0.38	0.80
step5	49.63	2.44	14.04	13.28	6.60	11.44	2.22	0.15	0.20	0.12	0.77	0.50	0.73	0.38	0.80
step10	49.64	2.55	13.87	13.66	6.37	11.28	2.26	0.16	0.21	0.12	0.76	0.50	0.73	0.38	0.79
step15	49.67	2.67	13.70	14.04	6.14	11.11	2.29	0.16	0.22	0.12	0.75	0.50	0.72	0.38	0.77
step20	49.69	2.79	13.52	14.43	5.91	10.94	2.32	0.17	0.23	0.12	0.73	0.50	0.72	0.38	0.76
step25	49.70	2.92	13.33	14.82	5.68	10.77	2.36	0.18	0.24	0.12	0.72	0.50	0.71	0.38	0.75
step30	49.74	3.05	13.14	15.22	5.45	10.56	2.39	0.19	0.26	0.12	0.71	0.50	0.70	0.38	0.74
step35	49.76	3.20	12.94	15.62	5.23	10.36	2.42	0.20	0.27	0.12	0.69	0.50	0.70	0.38	0.72
step40	49.78	3.35	12.73	16.03	5.00	10.16	2.46	0.21	0.28	0.12	0.68	0.50	0.69	0.38	0.71

subrtacted	wt.%
ol	3.89
pl	15.76
cp	13.12
total	32.77

sample	Rb (ppm)	Ba	Th	Nb	Sr	Zr	Y
AN-02	0.3	44	1.6	10	221	136	29
error	3.0	18	2.2	1	11	6	2
Final	0.4	61	2.4	15	220	199	42
error	4.4	25	3.2	2	11	9	3

	La (ppm)	Ce	Nd	Sm	Eu	Tb	Yb	Lu
KK-06	8.83	20.79	15.6	4.54	1.73	0.9	2.85	0.4
error	0.11	0.16	0.43	0.01	0.02	0.04	0.11	0.01
Final	12.37	29.3	21.85	6.344	2.131	1.26	4.03	0.566
error	0.154	0.226	0.602	0.014	0.025	0.056	0.156	0.014

fraction of melts and the bulk partition coefficient were calculated by using the result of subtracted percentage from major element calculation (fractional crystallization calculation from the most primitive basalt to one of the most evolved basalt; MgO = 5 wt.%). Fig. 4.8 shows the calculated results with the composition of the uncontaminated basalts. The results of calculation are in good agreement with the chemistry of the most evolved basalt. Consequently, a chemical trend of the uncontaminated basalts is readily explained by low pressure fractional crystallization process. All the uncontaminated basalts can be produced by fractional crystallization of the most primitive basalts. The most primitive basalt is, hereafter, called the pristine magma.

6. H_2O content of the pristine magma

The above discussion, that the compositional variation of the uncontaminated basalts can be explained by fractional crystallization at low pressure under dry condition, implicitly suggest that H_2O content of the pristine magma may not be significant. In order to confirm this, H_2O content of glass inclusions in olivine phenocrysts have been examined. One fresh basalt containing olivine, plagioclase and augite phenocrysts (NY-02-51) was selected. Groundmass is mostly basaltic glass. The sample has relatively low MgO content (5.6 wt.%) among the uncontaminated basalts. Olivine phenocrysts which contain measured glass inclusions are normally zoned with the core composition of $Fo_{67.3}$-$Fo_{68.3}$. The core compositions are considered to be in equilibrium with glass inclusions because Fe-Mg exchange partitioning coefficient between the core and the glass inclusion (Appendix C) is close to 0.3 (Roeder and Emslie, 1970). Major element compositions of glass inclusions are akin to those of groundmass basaltic glass. Analysis of olivine and glass inclusions was carried out with the JXA-8800R Electron Microprobe, using 15 kV accelerating voltage and 12 nA beam current. Counting time was 10 seconds. Beam size was 10 μm for glass analyses and 1 μm for olivine crystals.

At first, the sample was crushed into sub-mm size in an iron crusher. Olivine phenocrysts which have glass inclusions were collected by hand-picking. Next, the

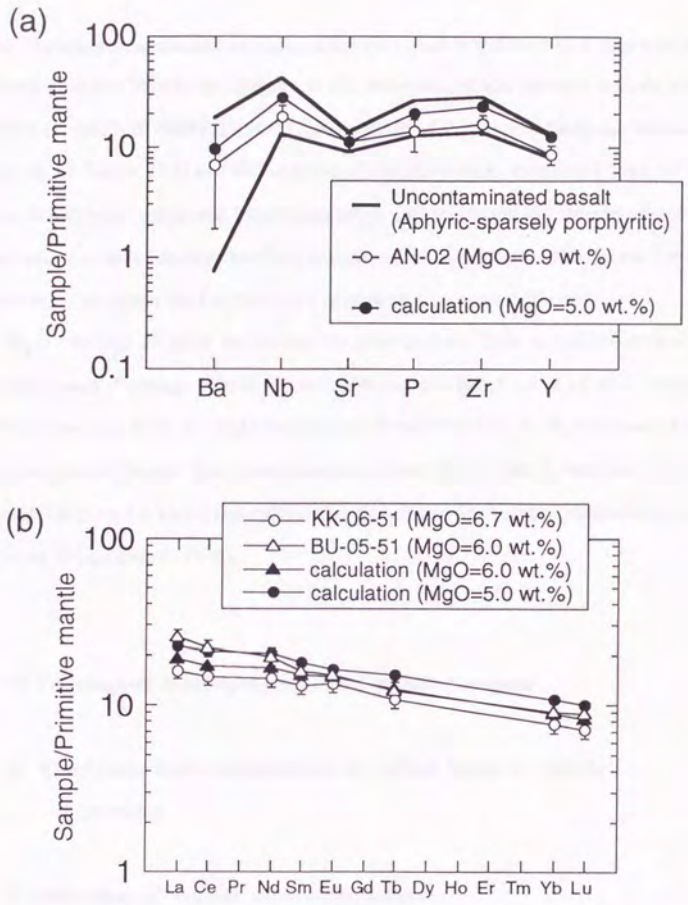

Fig. 4.8 Normalized patterns of (a) incompatible trace elements, (b) rare earth elements for aphyric rocks of the uncontaminated basalts, showing the effects of Rayleigh fractionation (shown as calculation). The average concentrations of MgO-rich (> 6.6 wt.%) uncontaminated basalts are also shown. All concentrations were normalized to the primitive mantle (McKenzie and O'Nions, 1991, 1995). Error bar: 2 sigma standard deviation of calibration line of XRF for (a), ±10 % for (b).